Miriam Wimmer-Teubenbacher, BSc

Improving Cytochrome P450 enzyme activity in Saccharomyces cerevisiae

MASTERARBEIT

zur Erlangung des akademischen Grades

Diplom-Ingenieurin

Masterstudium Biotechnologie

eingereicht an der

Technischen Universität Graz

Betreuer

Univ.-Prof. Dipl.-Ing. Dr.techn. Helmut Schwab

Institut für Molekulare Biotechnologie

Dipl.-Ing. Dr.techn. Anita Emmerstorfer, BSc

Graz, Juni 2014

EIDESSTATTLICHE ERKLÄRUNG

AFFIDAVIT

Ich erkläre an Eides statt, dass ich die vorliegende Arbeit selbstständig verfasst, andere als die angegebenen Quellen/Hilfsmittel nicht benutzt, und die den benutzten Quellen wörtlich und inhaltlich entnommenen Stellen als solche kenntlich gemacht habe. Das in TUGRAZonline hochgeladene Textdokument ist mit der vorliegenden Masterarbeit identisch.

I declare that I have authored this thesis independently, that I have not used other than the declared sources/resources, and that I have explicitly indicated all material which has been quoted either literally or by content from the sources used. The text document uploaded to TUGRAZonline is identical to the present master‘s thesis.

Datum / Date

Unterschrift / Signature

Danksagung

Ich möchte mich bei Herrn Univ.-Prof. Dipl.-Ing. Dr.techn. Helmut Schwab für die Möglichkeit eine Masterarbeit zu verfassen bedanken. Außerdem möchte ich mich für die anregenden Diskussionen während dem Institutsseminar bedanken.

Bei der Firma DSM möchte ich mich für das interessante Projekt und die fördernden Konferenzen bedanken. Außerdem möchte ich mich bei ACIB GmbH für meine Stelle als Diplomandin bedanken.

Ganz besonderer Dank gilt meiner Betreuerin Anita Emmerstorfer. Sie ist das Mastermind hinter dem *S. cerevisiae* Teils des CYP450 Projekts. Anita hat mir alle *S. cerevisiae* Arbeitstechniken beigebracht.

Danke an Harald Pichler, der mir gezeigt hat wie effektiv gutes Supervising sein kann. Mit seinem unerschöpflichen Fachwissen ist er uns immer zur Seite gestanden. Durch ihn bin ich überhaupt zu dieser Arbeitsgruppe gestoßen.

Besonderer Dank gilt meiner Arbeitsgruppe, den KollegInnen aus Labor 207. Tamara und Christine haben mir mit einigen Tipps und Tricks und wertvollem Wissen weitergeholfen. Ohne Sandra, Matthias, Eva und Sabine hätte ich sehr viel weniger Spaß und Unterhaltung während meiner Masterarbeit gehabt. Außerdem bin ich sehr dankbar für jede Kleinigkeit, die mir jemand von den vieren abgenommen hat.

Außerdem möchte ich mich bei Amneris bedanken, durch deren Magie das Laborgeschirr sauber, die Spitzen gesteckt und jederzeit ein paar aufmunternde Worte parat waren. Dass das HPLC nicht zertrümmert im Garten liegt, ist allein Thorsten, dem HPLC-Flüsterer zu verdanken.

Jedem der Leute aus den Häusern Petersgasse 12 und 14, die mich mit Rat und Tat unterstützten und auch mal zu einem Plausch bereit waren, möchte ich hiermit danken, speziell unserer erweiterten Arbeitsgruppe aus dem 3. Stock.

Auch möchte ich mich herzlich bei allen meinen Freunden bedanken, für offene Ohren und alle Schilderungen derer, die die Odyssee eines Studiums vor mir bestritten haben.

An dieser Stelle möchte ich meiner Schwägerin Carmen danken, die mir ihre Sprachkompetenz in Englisch zur Verfügung gestellt hat.

Auch sollen meine StudienkollegInnen nicht unerwähnt bleiben. Hausübungsteams, Lernallianzen und ein gelegentliches Heißgetränk haben mir vieles erleichtert.

Ich möchte mich bei meinen Eltern für den ehrlichen Glauben an mich und ihre Unterstützung bedanken. Großer Dank gilt auch meinen Großeltern, die wissen wie man Abschlüsse mit Stil feiert, mir immer sämtliche Daumen gedrückt haben und mir genauso bei meinem Studium geholfen haben wie sie bergsteigen.

Zu guter Letzt möchte ich meinem Mann Robert danke sagen. Worte können nicht beschreiben, wie dankbar ich dir für alles bin.

Abstract

Cytochrome P450 monooxygenases catalyze a huge variety of redox reactions, which renders this protein superfamily interesting biocatalysts for industrial applications. Eukaryotic Cytochrome P450 systems consists of the actual P450 enzyme and NADPH-cytochrome P450 reductase. Both enzymes are usually membrane-attached and one equivalent of NADPH is consumed for each oxygen atom introduced. To circumvent the need for tedious and time-consuming isolation of membrane-bound proteins and for addition of NADPH, biocatalysis employing cytochrome P450 systems is frequently performed with whole cells. *Saccharomyces cerevisiae* is an established host for heterologous protein expression and provides ample of endoplasmic reticulum membrane space for cytochrome P450 expression – particularly if compared to *E. coli* hosts. We have chosen three different P450 enzymes and their suitable NADPH-cytochrome P450 reductases to be tested in whole-cell conversions. Cytochrome P450 performance was improved by metabolic engineering and optimization of the cultivation conditions.

Kurzfassung

Cytochrom P450 Monooxygenasen katalysieren eine große Bandbreite an Redoxreaktionen. Deswegen sind die Mitglieder dieser Protein-Superfamilie interessante Biokatalysatoren für industrielle Anwendungen. Eukaryotische P450 Systeme bestehen aus dem tatsächlichen P450 Enzym und einer NADPH-Cytochrom P450 Reduktase. Beide Enzyme sind häufig membrangebunden und verbrauchen pro integriertem Sauerstoffatom ein Äquivalent NADPH. Um die schwierige Isolierung von membrangebundenen Proteinen und die Zugabe von NADPH zu vermeiden, wird Cytochrom P450-basierte Biokatalyse üblicherweise mit ganzen Zellen durchgeführt. *Saccharomyces cerevisiae* ist ein etablierter Wirtsorganismus für die heterologe Proteinexpression und stellt – vor allem im Vergleich zu *E. coli* - ausreichend Membranen des Endoplasmatischen Retikulums für die Proteinverankerung zur Verfügung. Im Rahmen dieser Arbeit wurden drei verschiedene P450 Enzyme und ihre passenden NADPH-Cytochrom P450 Reduktasen ausgewählt und in Ganz-Zellumsetzungen angewandt. Mittels Metabolic Engineering und optimierter Kultivierungsmethoden wurde die Verbesserung der Cytochrome P450 Funktionalität erreicht.

TABLE OF CONTENTS

1. ABBREVIATIONS

Abbreviation	Name
At	*Arabidopsis thaliana*
CDW	cell dry weight
cPCR	colony PCR
CPR	NADPH-cytochrome P450 reductase
CWW	cell wet weight
CYP450	cytochrome P450 enzyme
ddH_2O	double-distilled H_2O
DMSO	dimethylsulfoxid
FAD	flavin adenine dinucleotide
FDA	U S Food and Drug Administration
FMN	flavin mononucleotide
FPPS	farnesyl diphosphate synthase
GC-FID	gaschromatograph with flame ionisation detector
hCPR	human NADPH-cytochrome P450 reductase
HPLC-MS	high pressure liquid chromatography with mass-spectrometry detector
HPO	*Hyoscyamus* premnaspirodiene oxygenase
HSP	Heat Shock Protein
KP_i	potassium phosphate buffer
LB	lysogeny broth
LimS	(-)-limonene synthase
NADPH	nicotinamide adenine dinucleotide phosphate
OD_{600}	optical density at 600 nm
ONC	overnight culture
P450	cytochrome P450 enzyme
PCR	polymerase chain reaction
PM17	(4S)-limonene-3-hydroxylase
SD	synthetic defined medium; yeast minimal medium
SDS	sodiumdodecyl sulfat
TBS	tris-buffered saline
TBST	tris-buffered saline and Tween 20
ValS	(+)-valencene synthase
YPD	yeast peptone dextrose complete medium

2. INTRODUCTION

2.1 CYTOCHROME P450 ENZYMES

Cytochrome P450 enzymes (CYP 450) are named for their distinctive absorption band at 450 nm in their reduced carbon-monoxide bound form [1]. CYP450s contain a heme group and the fifth ligand of the heme iron is a cystein thiolate group. This makes CYP450s heme thiolate proteins and is responsible for the absorption band at 450 nm. Usually, the terminology of enzymes is based on their function, but enzymes within this large and old superfamily, are able to catalyse a huge variety of different reactions. Basically, CYP450 enzymes are external monooxygenases, which catalyse the transfer of molecular oxygen to X-H bonds (X:-C, -N, -S) of a substrate, while the other oxygen atom is reduced to water [1]. Within the CYP450 superfamily, the structural fold and topology are strongly conserved, whereas, the substrate recognition sites are variable. This indicates that members of this superfamily share a common mechanism of oxygen activation and are able to catalyse a wide range of reactions due to different substrate binding sites. . Examples for the range of reactions are hydroxylations, peroxidations, deaminations and dealkylations. Depending on the organism, P450s take part in important processes such as carbon source assimilation, degradation of xenobiotics, the biosynthesis of hormones and defence substances. Due to their versatility and stereoselectivity CYP450 enzymes are valued biocatalysts for industrial purposes [1].

According to Bernhardt et al. (2007), 10 classes of P450 enzymes exist. This Master's thesis deals with three enzymes from class *II*. Class *II* cytochrome P450s are most commonly found in eukaryotes. The monooxygenase system consists of two integral membrane proteins found in the endoplasmic reticulum, the CYP450 enzyme and the NADPH-cytochrome P450 reductase (CPR).

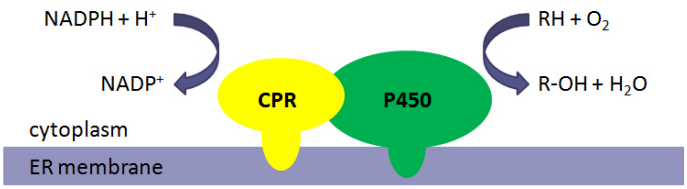

Figure 1: Schematic organization of class II P450 monooxygenase systems

CPR belongs to a family of diflavin reductases, which contain both FAD and FMN [2]. These cofactors catalyse the electron transfer reaction. Diflavin reductases were formed when during evolution the genes of FMN-containing flavodoxin and a FAD-binding ferredoxin $NADP^+$ reductase were fused. Structural analysis confirmed two independent folding units linked by a flexible peptide hinge [2]. The direction of the electron flow is from NADPH to FAD, to FMN and finally to the CYP450 heme. First, NADPH binds near the FAD cofactor and transfers two electrons in the form of a hydrid ion to the N5 of FAD. FAD is reduced to protonated hydroquinone $FADH_2$. Next, the two electrons are transferred to FMN, which is reduced to $FMNH_2$. To release $NADP^+$ a second NADPH has to bind, which transfers another hydride ion. This leads to a CPR with both cofactors in the hydroquinone state ($FADH_2$, $FMNH_2$). Last but not least, the two electrons are transferred to the iron of the P450 heme-thiolate complex [2]. Figure 2 displays the electron chain in CPR enzymes.

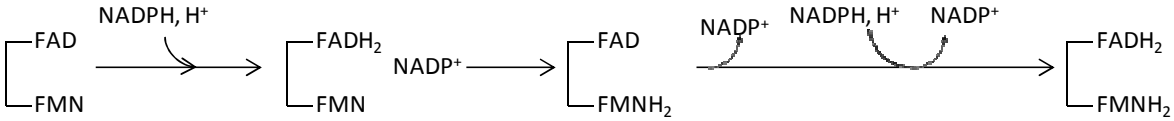

Figure 2: Electron transfer chain in CPR

The catalytic cycle in P450 enzymes begins with substrate binding [3]. In this step, the substrate removes the water molecule in axial position, which causes the iron to leave the plane of the porphyrin ring. This event leads to the first electron transfer from CPR to the P450 heme, which results in the reduction of Fe^{III} to Fe^{II} (ferrous state). The next step is the binding of oxygen in which the dioxygen complex of P450 is formed. In this step, an electron from iron(II) and another from the oxygen pair form a Fe^{III}-O_2 bond. Now the second electron from CPR is transferred to the complex and creates an iron(III)-peroxo complex. This complex is protonated to form the iron(III)-hydroperoxo complex (Fe^{III}-OOH). The second protonation step results in the elimination of a water molecule forming on iron(V)-

oxo species. Finally, the oxygen from iron(V)-oxo is introduced into the X-H bond of the substrate. There are two possible reaction mechanisms which are suggested for the introduction: a concerted mechanism or a cage controlled radical mechanism. The release of the product and binding of a new substrate initiates the catalytic cycle again [3]. The catalytic cycle of P450 enzymes is shown in Figure 3.

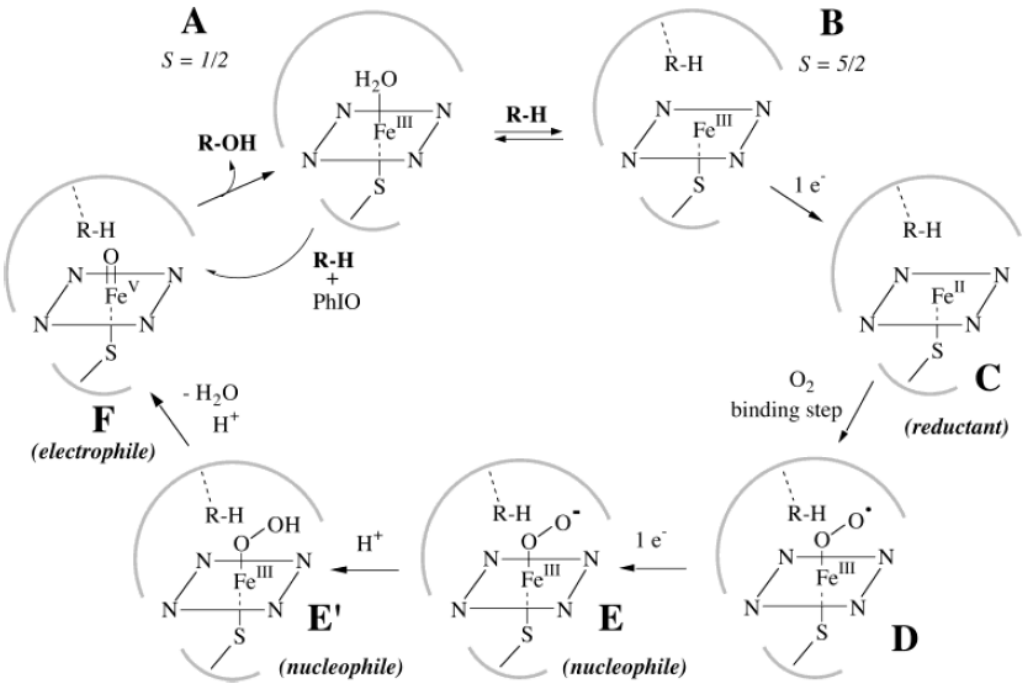

Figure 3: Catalytic cycle of P450 enzymes [3]

2.1.1. *HYOSCYAMUS MUTICUS* PREMNASPIRODIENE OXYGENASE

Hyoscyamus muticus premnaspirodiene oxygenase (HPO) originating from Egyptian henbane may play an important role in the synthesis of solavetivone, which is a sesquiterpene phytoalexin [4].

HPO is also able to hydroxylate (+)-valencene, another sesquiterpene, at C2 to generate trans-nootkatol, which can subsequently be oxidised to nootkatone (Figure 4).

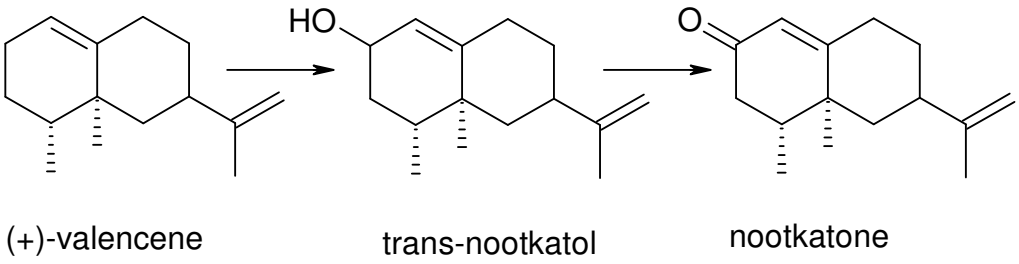

Figure 4: Conversion of (+)-valencene to nootkatone, hydroxylation is catalysed by HPO, conversion to nootkatone is catalysed by a dehydrogenase

(+)-Valencene is a fragrance of oranges and is very cheap due to its abundance [5]. Nootkatone, on the other hand, is a high value fragrance of grapefruits and is greatly demanded by the food and cosmetic industry. To provide optimal supply with redox equivalents, HPO is co-expressed with *Arabidopsis thaliana (At)* CPR from.

2.1.2. LIMONENE HYDROXYLASE

(4S)-Limonene-3-hydroxylase (isoform PM17) originates from peppermint (*Mentha x piperita*) and converts (-)-limonene to (-)-trans-isopiperitenol by adding a hydroxyl-group at C3 [6]. Both, (-)-limonene and isopiperitenol are precursors of (-)-menthol. (-)-Menthol is one of the essential oils in mint and is responsible for the minty flavour [7]. It is used in candy, chewing gum and in cold medications. The use in the last case is due to an effect that (-)-menthol has on sensory nerves in the upper air passages. (-)-Menthol induces thirst and the drive to breathe.

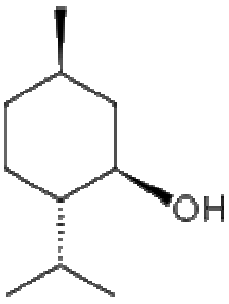

Figure 5: Chemical structure of (-)-menthol

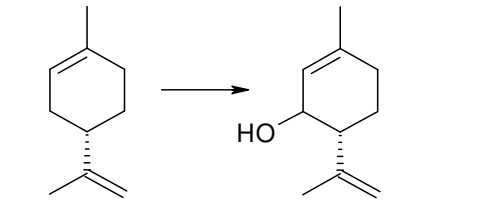

(-)-limonene (-)-trans-isopiperitenol

Figure 6: Hydroxylation of (-)-limonene to (-)-trans-isopiperitenol by PM17

(-)-Limonene is a monoterpene and (-)-menthol and isopiperitenol are oxygenated monoterpenes, contributing to the fragrance and flavour of peppermint. (-)-Limonene strongly smells like oranges and is found in the zest of both, oranges and lemons. Similar to (+)-valencene, (-)-limonene is readily available and, therefore, rather cheap. In contrast, isopiperitenol is one of the fragrances of lemongrass and is of high demand as well. As HPO, PM17 is co-expressed with *At*CPR.

2.1.3. CYP2D6

Cytochrome P450s play an important role in the clearance of drugs and xenobiotics in the human liver [8]. They catalyse phase 1 of the metabolic clearance by introducing oxygen into the substrate to make it more water soluble. CYP2D6 makes up roughly 2% of all CYP450s expressed in the liver, but is involved in the metabolism of 25% of drugs used currently. The FDA stated in 2008 that metabolites of drugs have to be tested in toxicity studies. It is very difficult to achieve the stereo- and regioselective hydroxylation of a non-activated carbon by chemical syntheses, which is needed to produce drug metabolites. Hence, drug metabolites are synthesised biocatalytically with recombinant enzymes such as CYP2D6.

One of the drugs metabolized by CYP2D6 is bufuralol, which is a widely used β-blocker [9]. Bufuralol is hydroxylated to 1-hydroxybufuralol (Figure 7).

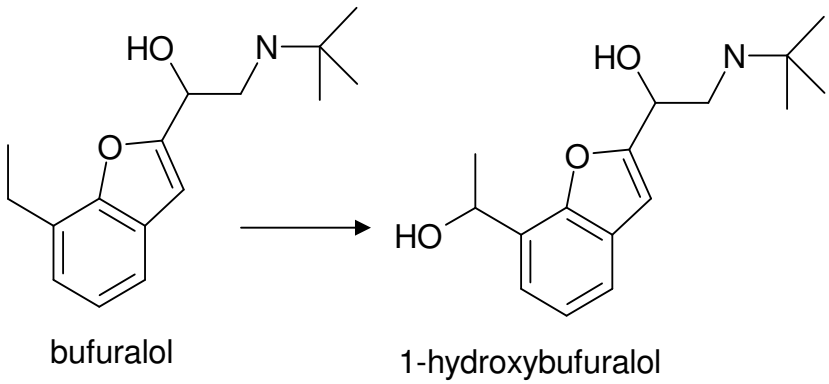

Figure 7: Conversion of bufuralol to 1-hydroxybufuralol catalysed by CYP2D6

As CYP 2D6 is a human enzyme, it is co-expressed with human CPR (hCPR) to provide optimal supply of redox equivalents, thus ensuring best possible conditions for catalytic activity.

2.2 WHOLE CELL HYDROXYLATIONS

The chemical introduction of oxygen atoms is often unspecific and requires the involvement of toxic and expensive reagents [10]. Therefore, enzymes, which work under mild conditions are applied to catalyse chemo-, enantio- and regioselective hydroxylations. Usually, chemists prefer partially purified enzyme preparations due to easier handling in comparison to whole cell biocatalysts. The purification of enzymes is expensive and not feasible for all enzymes. The isolation of functional membrane attached-proteins is particularly difficult. In most cases, the extraction of such enzymes from the membrane leads to loss of activity. Additionally, class *II* cytochrome P450 enzymes need another membrane bound enzyme, CPR, to be provided with electrons for the reaction. Another problem poses the supply with NADPH, which can be easily solved by using the metabolism of whole cells. In general, cells provide protection from shear stress and a natural environment for the enzymes. Whole cells can be applied as biocatalysts, if intracellular enzymes do not interfere with the synthesis of the product and do not convert it further.

2.3 *SACCHAROMYCES CEREVISIAE* AS EXPRESSION HOST

S. cerevisiae and *E. coli* are very well studied expression hosts. Both microorganisms have been used to express various proteins, even membrane attached enzymes as CYP450s [11]

[12], [13]. At the very beginning of this project, HPO was expressed in *E. coli* [12]. High expression levels could be detected via Western blot but the activity was too low for industrial applications. Hence, it was concluded that inclusion bodies were formed due to hydrophobic domains of the enzyme. *E. coli* only provides the cytoplasmic membrane where membrane proteins can attach to. Huge amounts of recombinant enzymes attached to the cytoplasmic membrane can lead to reduced viability and stability of the cells [12]. Therefore, *S. cerevisiae* was chosen as alternative expression host. As a eukaryote, *S. cerevisiae* cells maintain various membranes, especially the ER membrane where CPR, HPO, PM17 and CYP 2D6 can be anchored. Additionally, the cells provide cellular features similar to mammalian or plant cells, which make the correct folding of the target enzymes easier compared to *E. coli* [15]. Another advantage of *S. cerevisiae* is the heat shock response. The protein concentration in the cytosol at 300 mg/mL is very high and poses a folding and aggregation problem [16]. Therefore, the cytoplasm holds a large variety of Heat Shock Proteins (HSPs). Proteins of the HSP 100, 90, 70 and 40/J families are present as unfoldases and anti-aggregases. The lumen of the ER provides a folding environment for proteins. In contrast to the cytosol, only a small number of HSPs is exhibited by the ER lumen. For example, members of the HSP 70 family like Kar2p and Lhs1p, HSP 40 proteins, protein disulfide isomerase and Cne1p, which is involved in the folding of glycosylated proteins [16].

2.4 AIMS OF THIS MASTER`S THESIS

My participation in the CYP450 project at ACIB started during the final year of the project. Thus, many achievements had been done before. My role was to find improvements affecting all three CYP450 systems, i.e. HPO-, PM17- and CYP2D6/CPR. The major aim of this Master's thesis was to improve CYP450 activity in *S. cerevisiae*. To reach this goal, two different approaches were chosen. Either, cells were metabolically engineered and tested for better substrate conversions, or, assay conditions were modified. In the former case, various *S. cerevisiae* knock-out strains from the EUROSCARF [17] collection were chosen to be tested in P450 activity assays with resting cells. Some of these strains showed decreased activity levels. We concluded that the eliminated genes might be beneficial for activity or expression of membrane-attached enzymes in general or for CYP450 enzymes in particular.

Therefore, over-expression strains were constructed with the target genes under control of the galactose inducible promoter P_{GAL1} to be tested in P450 activity assays.

The following genes were tested during this Master's thesis: *DAP1*, *ICE2*, *KAR2*, *LHS1*, *MXR*1, *RAD52* and *SUR2*. In previous (+)-valencene conversion assays, the over-expression of *DAP1*, *ICE2* and *SUR2* has led to higher conversion rates [14]. Dap1p is a heme-binding, damage response protein, which is involved in the regulation of Erg11p, which is an endogenous yeast cytochrome P450 enzyme [18]. Sur1p is a mannosylinositol phosphorylceramide synthase catalytic subunit, which forms a complex with Csg2p [19]. This complex is involved in sphingolipid biosynthesis. In *S. cerevisiae*, sphingolipids and ergosterol form microdomains in the plasma membrane which take part in the sorting of membrane proteins and lipids. Ice2p is an integral ER membrane protein, which is supposedly involved in cellular zinc ion homeostasis and in ER inheritance from mother to daughter cells [20]. Overexpressing *RAD*52 in *P. pastoris* increased P450 activity in HPO, PM17 and CYP2D6/CPR systems [21]. Rad52p is involved in the repair of double strand breaks in DNA, maintenance of telomere length and mating type switching [22]. Kar2p and Lhs1p are both heat shock response chaperones [23], [24]. Mxr1p is a methionene-S-sulfoxide reductase which protects iron-sulfur clusters from oxidative inactivation [25].

Another objective of this Master`s thesis was to generate strains expressing (-)-limonene synthase (LimS) for *in vivo* (-)-limonene synthesis in *S. cerevisiae*. This measure may circumvent problems with phase transfer hampering the conversion of (-)-limonene to isopiperitenol. (-)-Limonene is produced from geranyldiphosphate, which is a product of the mevalonate pathway. The bottleneck of this pathway is Hmg1p, a membrane attached enzyme regulated by feedback inhibition [26]. By truncating the membrane domains of *HMG1*, the regulatory effect is abolished. Therefore, sufficient farnesyl diphosphate is available for (+)-valencene synthesis. This approach has been successfully applied for (+)-valencene synthesis in *S. cerevisiae* [14]. Farnesyl diphosphate synthase (FPPS), Erg20p in *S. cerevisiae*, synthesises farnesyl diphosphate in two condensation reactions from two molecules isopentenyl diphosphate and one molecule of dimethylallyl diphosphate [27]. Geranyl diphosphate is formed in the first condensation reaction out of isopentenyl diphosphate and dimethylallyl diphosphate. The second condensation generates farnesyl diphosphate from geranyl diphosphate and another isopentenyl diphosphate moiety.

3. MATERIALS AND METHODS

3.1 MEDIA AND BUFFERS

Table 1: Media and buffer compositions used in this thesis

Media/Buffer	Composition
(-)-limonene stock (100 mM)	70.9 mg (-)-limonene, 5 mL DMSO, 50 µL Triton™-X100
(+)-valencene stock (100 mM)	105.4 mg (+)-valencene, 5 mL DMSO, 50 µL Triton™-X100
10x TBS	30.3 g Tris (0.25 M), 87.6 g NaCl (1.5 M), pH adjusted with 1 M HCl to pH 7.5, to 1 L with H_2O
20x Transfer buffer (Western blot)	14.5 g Tris (0.24 M), 72 g glycin (1.92 M), to 500 mL with H_2O
50x TAE buffer	242 g Tris dissolved in 600 mL H_2O, 57.1 mL glacial acetic acid and 100 mL of 0.5 M EDTA, to 1 L with H_2O
ampicillin Stock (amp), (100 µg/mL)	100 mg/mL in H_2O
dropout powder (-histidine)	1 g L-adenine, 1 g L-lysine, 1 g L-tyrosin, 1 g uracile, 1 g L-tryphtophan, 1 g L-leucine
dropout powder (-histidine-uracil)	1 g L-adenine, 1 g L-lysine, 1 g L-tyrosin, 1 g L-tryphtophan, 1 g L-leucine
dropout powder (-trypthophan)	1 g adenine, 1 g L-lysine, 1 g L-tyrosin, 1 g L-histidine, 1 g uracile, 1 g L-leucine
dropout powder (-uracil)	1 g adenine, 1 g L-Lysine, 1 g L-Tyrosin, 1 g L-histidine, 1 g L-tryphtophan, 1 g L-leucine
galactose raffinose stock	35 g raffinose, 100 g galactose, to 500 mL with H_2O
geneticin stock	100 mg/mL in H_2O
LB-agar	20 g LB powder and 20 g agar to 1 L H_2O
LB-amp-agar	20 g LB powder and 20 g agar to 1 L H_2O, 1 mL amp-stock added after autoclaving
MOPS buffer	209.3 g MOPS dissolved in 1 L H_2O
Ponceau S solution	0.1 % Ponceau S in 5 % acetic acid
Potassium phosphate buffer (KP_i buffer, 1 M, pH 7.4)	177.99 g Na_2HPO_4*2 H_2O dissolved in 1 L H_2O 136.09 g KH_2PO_4 dissolved in 1 L H_2O 802 mL of 1 M Na_2HPO_4 plus 198 mL of 1 M KH_2PO_4
Resuspension solution (Riezmann) [28]	0.799 g NaOH dissolved in 10 mL ddH_2O 9.25 mL of 1.75 M NaOH plus 0.75 mL of β-mercaptoethanol
Sample buffer (Riezmann) [28]	66 µL NuPage® Sample Buffer, 33 µL of 1 M

	Tris, 2 µL of β-mercaptoethanol
SD-agar	6.7 g bacto yeast nitrogen base, 1 g dropout powder, 0.1 g NaOH, 20 g agar, to 800 mL with H_2O 20 g glucose, in 200 mL H_2O autoclaved separately
SD-media	6.7 g bacto yeast nitrogen base, 1 g dropout powder, 0.1 g NaOH, to 1 L with H_2O 20 g glucose, to 200 mL H_2O autoclaved separately
SD-ura galactose	6.7 g bacto yeast nitrogen base, 1 g dropout powder, 0.1 g NaOH, to 900 mL with H_2O 100 mL galactose/raffinose stock added
SOC-media	20 g bacto tryptone, 0.58 g NaCl, 5 g bacto yeast extract, 2 g $MgCl_2$, 0.16 g KCl, 2.46 g $MgSO_4$, 3.46 g dextrose, to 1 L with H_2O
TBST	999.7 mL 1x TBS, 0.3 mL Tween20
TBST-milk	2.5 mL dry milk powder dissolved in 50 mL TBST
Transfer solution (Western blot)	50 mL 20x Transfer buffer, 100 mL methanol, to 1 L with H_2O
YPD-agar	20 g peptone, 10 g yeast extract, 20 g agar, to 900 mL with H_2O 20 g glucose, to 100 mL with H_2O autoclaved separately
YPD-geneticin-agar	20 g peptone, 10 g yeast extract, 20 g agar, to 900 mL with H_2O 20 g glucose, to 100 mL with H_2O autoclaved separately 1 mL geneticin stock added after autoclaving
YPD-media	20 g peptone, 10 g yeast extract, to 900 mL with H_2O 20 g glucose, to 100 mL with H_2O autoclaved separately

3.2 REAGENTS

Table 2: Reagents used in this thesis

Reagent	Supplier
(-)-limonene	DSM Pharma Chemicals, The Netherlands
(+)-valencene	DSM Pharma Chemicals, The Netherlands
agarose LE	Biozyme, Germany
ampicillin	Sigma-Aldrich, Germany
aqua bidest. (ddH_2O)	Fresenius Kabi GmbH, Austria
bufuralol	Sigma-Aldrich, Germany
dimethylsulfoxide (DMSO)	Roth GmbH, Germany
dNTPs	Promega Corporation, USA
dream Taq Polymerase [5 U/µL]	ThermoScientific, USA
dry milk powder	Low fat milk powder, bought in a local supermarket
fructose	bought in a local pharmacy
galactose	Roth GmbH, Germany
Gene Jet™ Plasmid Miniprep Kit	ThermoScientific, USA
glucose	Roth GmbH, Germany
glycerol	Roth GmbH, Germany
L-/D-lactic acid	Roth GmbH, Germany
L-amino acids, varios	Roth GmbH, Germany
LB (Luria-Bertani) Lennox	Roth GmbH, Germany
lithium acetate	Roth GmbH, Germany
n-Hexadecane	Roth GmbH, Germany
NuPage® LDS Samples Buffer (4x)	Invitrogen, USA
phenylmethylsulfonyl fluoride (PMSF)	Sigma-Aldrich, Germany
Ponceau S ($C_{22}H_{16}N_4O_{13}S_4$)	Sigma-Aldrich, Germany
potassium cyanide (KCN)	Sigma-Aldrich, Germany
potassium hydrogen phosphate (KH_2PO_4)	Roth GmbH, Germany
prednisolone	Roth GmbH, Germany
primary antibodies (Anti-c*myc*-Ab rabbit and Anti-FLAG-Ab Mouse)	Sigma-Aldrich, USA
raffinose	Roth GmbH, Germany
restriction Enzymes and adequate buffers, various	ThermoScientific, USA
secondary antibodies (Anti-Rabbit IgG ab Anit-Mouse)	Sigma-Aldrich, USA
single stranded carrier DNA	Sigma-Aldrich, Germany
sodium dithionite ($Na_2S_2O_4$)	Riedel de Haen, Germany
sodium hydroxide (NaOH)	Roth GmbH, Germany
sorbitol	Roth GmbH, Germany
SuperSignal® West Pico Chemiluminescent Substrate	ThermoScientific, USA
T4 DNA Ligase [10 U/µL]	ThermoScientific, USA

Tris	Roth GmbH, Germany
Tween20	Roth GmbH, Germany
uracil	AppliedChem GmbH, Germany
Wizard® SV Gel and PCR Clean Up System	Promega Corporation, USA
yeast extract	Roth GmbH, Germany
β-mercaptoethanol	Sigma-Aldrich, Germany

3.3 STRAINS

Table 3: Purchased strains

Organism	Strain	Genotype	Source
E. coli	Top10F´	F{*lac*I^{q} Tn*10* (Tet^{R})} *mcr*A Δ(*mrr-hsa*RMS-*mcr*BC) Φ80 *lac*ZΔM 15 Δ*lac*X74 *rec*A1 *ara*D139 Δ(*ara-leu*)7697 *gal*U *gal*K *rps*L *end*A1 *nup*G	Invitrogen, USA
S. cerevisiae	W 303 *MATa/MATα*	{*leu2-3,112 trp1-1 can1-100 ura3-1 ade2-1 his3-11,15*} [*phi*$^{+}$]	ThermoScientific, USA

Table 4: Formerly constructed strains

strain	source
S. cerevisiae W303 *MATα* P_{GAL1}-*DAP1*	Anita Emmerstorfer [14]
S. cerevisiae W303 *MATα* P_{GAL1}-*ICE2*	Anita Emmerstorfer [14]
S. cerevisiae W303 *MATα* P_{GAL1}-*SUR1*	Anita Emmerstorfer [14]
S. cerevisiae W303 *MATa* leu2::P_{PGK}-t*HMG1*	Anita Emmerstorfer [14]
S. cerevisiae W303 *MATα* P_{GAL1}-*KAR2*His_6	Anita Emmerstorfer [14]
S. cerevisiae W303 *MATα* P_{GAL1}-*LHS1*His_6	Anita Emmerstorfer [14]
S. cerevisiae W303 *MATα* P_{GAL1}-*MXR1*His_6	Anita Emmerstorfer [14]
S. cerevisiae W303 *MATα* P_{GAL1}-*RAD52*His_6	Anita Emmerstorfer [14]

3.5 PRIMER

Table 5: Primers used in this thesis

Primer	5'-3'
Fw(start_Gal1)	ACGGATTAGAAGCCGCCGAG
R1(Ice2)	GTATTTCACCTTCCTTTTTGTCTTCGCGTATTTGGCAAAGGAATTCGAGCTCGTTTAAAC
F1(Ice2_350)	AATTATACCACCGTCTCACTGAACCAATGCCGGATCCCCGGGTTAATTAA
Rv(Ice2)	GATTGGAATTGAAAGTAGTG

3.6 INSTRUMENTS AND DEVICES

Table 6: Instruments and devices used in this thesis

Task	Instrument/Device	Manufacturer
Centrifuge	Avanti™ Centrifuge J-20 XP Rotor JA-10 Rotor JA-25,5	Beckman Coulter, USA
Determination of DNA concentration	NanoDrop 2000c Spectrophotometer	Thermo Scientific, USA
Electrotransformation	MicroPulser™ Electroporation Cuvettes (2 mm gap)	BIO-RAD, USA Molecular BioProducts Inc., USA
GC-FID	Hewlett Packard 6890 Series with a FID detector Agilent 19091J-141 (Capillary 10.0 m x 0.1 mm x 0.1 µm film)	Agilent Technologies, USA
Gel electrophoresis	PowerPac™ Basic SUB-Cell® GT GelDoc-It™ Imaging System	BIO-RAD, USA BIO-RAD, USA UVP, USA
HPLC-MS	Agilent technologies 1200 Series, MSD SL detector with electrospray ionization unit XDB-C18 (column, 1.8 µm, 4.6 x 50 mm)	Agilent Technologies, Austria
Incubator (30, 37°C)	Binder Kühlbrutschränke	Binder GmbH, Germany
Mixing small volumes	Vortex-Genie 2	Scientific Industries Inc., USA
OD Measurement	BioPhotometer Cuvettes (10x4x45 mm)	Eppendorf, Germany Sarstedt, Germany
PCR reaction	GeneAmp®PCR System 2700	Applied Biosystems, USA
Plate reader	POLARstar Galaxy	BMG Labtech GmbH, Germany
Shaker	Multitron	Infors-HT, Switzerland
Shaker for small volumes	Thermomixer comfort	Eppendorf, Germany
Table-top centrifuge	Microcentrifuge 5415R	Eppendorf, Germany
Ultracentrifuge	Optima™ LE-80K Ultracentrifuge Rotor SW 41 41,000 RPM	Beckman Coulter, USA
Western Blot	XCell *SureLock*™ Mini-Cell Nitrocellulose membrane, Hybond-ECL™ G:Box HR	Invitrogen, USA Amersham Biosciences, Sweden Syngene, UK

3.7 PLASMIDS

Table 7: Plasmids used in this Master´s thesis

Plasmid	Source
pESC-*URA3*	Agilent Technologies, USA
pESC *URA3* P_{GAL1}-CPR-*myc* P_{GAL1}-PM17 opt.-Flag	Anita Emmerstorfer [14]
pYES2 P_{GAL1}-CPR-*myc* P_{GAL1}-HPO-Flag	Anita Emmerstorfer [14]
pFA6a *TRP1* P_{GAL1}-*ICE*2His_6	Anita Emmerstorfer [14]
pRS413 P_{GPD}-LimS opt.	Anita Emmerstorfer [14]
pESC *URA3* P_{GAL1}-CPR-*myc* P_{GAL1}-PM17 opt.-Flag	Anita Emmerstorfer [14]
pESC *URA3* P_{GAL1}-hCPR-*myc* P_{GAL1}-CYP2D6-Flag	this work

3.8 SYNTHETIC GENES

Table 8: Synthetic genes used in this thesis

Gene	Source
hCPR opt.	Tamara Wriessnegger, purchased from GeneArt®
CYP2D6 opt.	Tamara Wriessnegger, purchased from GeneArt®

3.9 GENERAL METHODS

Electrotransformation

One-two µL of plasmid solution were mixed with 50 µL of electrocompetent *E. coli* cells in electroporation cuvettes on ice. For the electroporation program, Eco2 was used (pulsed for 5-6 ms at 2.5 kV). One mL of SOC medium was added, the mix was transferred into sterile microfuge tubes and incubated at 37°C, 650 rpm for 30 min. Cells were pelleted and streaked out onto LB-amp.

Lithium acetate Transformation

Five mL of YPD medium were inoculated and incubated at 30°C with shaking overnight (overnight culture ONC) was used to inoculate 50 mL of YPD medium to an OD_{600} of 0.1. Cells were incubated at 30°C and 130 rpm to an OD_{600} of 0.2 to 0.5 (3-5 h), transferred into a sterile 50 mL centrifuge tube and were centrifuged at 2,500 rpm for 5 min [29]. The

supernatant was discarded, cells were resuspended in 25 mL ddH_2O and centrifuged at 2,500 rpm for 5 min. Supernatant was discarded, cells were resuspended in 300 µL of 100 mM lithium acetate and transferred to a sterile 1.5 mL microfuge tube. Single-stranded carrier DNA (2 mg/mL) was boiled at 95°C for 5 min and quickly chilled on ice. Fifty µL aliquots of resuspended cells were transferred into microfuge tubes, pelleted and lithium acetate was removed with a micropipette.

The single reagents of the transformation mix were added in the following order:

Table 9: transformation mix

polyethylene glycol, 50 % in H_2O	240 µL
lithium acetate 1M	34 µL
single stranded carrier DNA	5 µL
plasmid DNA or knock-in/knock-out cassette	25-50 µL

After the addition of all components of the transformation mix, the mixture was stirred gently with a pipette for 30 s. Cells were incubated at 30°C for 30 min, heat-shocked at 42°C for 20 min, pelleted at 7,000 rpm for 15 s and the transformation mix was removed with a micropipette. The cell pellet was resuspended in 1 mL of pre-warmed (30°C) YPD medium, incubated at 30°C and 650 rpm for 1 h, pelleted, resuspended in 200 µL of ddH_2O and streaked out onto selective synthetic deficiency (SD) agar.

Plasmid isolation

Plasmid isolation followed the GeneJET™ Plasmid Miniprep Kit quick protocol. The elution step was carried out with 100 µL of ddH_2O.

DNA Restriction

For restriction of DNA, 40 µL sample, 7 µL of buffer, 21 µL of ddH_2O and 2 µL of total restriction enzyme were mixed and incubated at 37 °C for a minimum of 3 h or overnight. Two enzymes using the same buffer could be used in the same mixture; others could be applied one after another with a purification step in between.

For restriction analysis, 2 µL of DNA-solution, 1 µL of Fast Digest green buffer (10x), 6 µL of ddH_2O and 1 µL of enzyme were mixed and incubated at 37°C for 15 min.

DNA Ligation

Vector and insert were ligated at a molar ratio of 1:3. Calculation of amounts needed was done with the online *in silico* ligation calculator (http://www.insilico.uni-duesseldorf.de/Lig_Input.htmL). 1.5 µL of T4 ligase buffer (10x), 0.5 µL of T4 ligase and ddH_2O were added to a final volume of 15 µL. The ligation mix was incubated at room temperature for 30 min and heat-shocked at 65°C for 5 min. Solutions were immediately used for electrotransformation or stored at -20°C.

DNA Gel purification

DNA-fragments were separated via gel electrophoresis. Samples were loaded onto agarose gels (1% agarose in TAE buffer), separated at 90 V and purified according to the Promega Wizard® SV GEL and PCR Clean-UP System manual. Fifty µL of ddH_2O were used for DNA eluation.

Electrocompetent cells

Single, fresh colonies from LB plates were used to inoculate 30 mL of LB media and incubated at 37°C, 220 rpm overnight. Five mL of overnight culture were used to inoculate 500 mL of LB media in 2 L baffled flasks. Cells were incubated at 37°C, 170 rpm until they reached an OD_{600} between 0.6 and 0.7. Cells were chilled on ice for 30 min, centrifuged in 500 mL sterile, prechilled centrifuge bottles at 2,000 x g and 4°C for 15 min and resuspended in 500 mL of ice-cold ddH_2O. The centrifugation step was repeated, the cell pellet was resuspended in 35 mL ice-cold 10% glycerol and centrifuged at 4,000 x g and 4°C for 15 min. The supernatant was discarded and the pellet was resuspended in 1 mL of pre-chilled, sterile 10% glycerol. Eighty µL aliquots were transferred to 1.5 mL Eppendorf tubes and chilled on ice for immediate use or stored at –80°C.

Colony PCR

A small amount of cells from a single colony was resuspended in 50 µL ddH_2O, boiled at 95°C for 5 min and pelleted. The mixture for colony PCR was as follows: 15.75 µL ddH_2O, 2.5 µL

10 x DreamTaq buffer, 2.5 µL dNTPs, 1 µL forward and reverse primer each, 2 µL of colony supernatant and 0.25 µL DreamTaq polymerase.

PCR settings: 95°C (4 min) 30 x [95°C (30 s) – XX°C(30 s) – 72°C (1 min)] 72°C (7 min); annealing temperature depended on primers.

3.10 CYP450 Activity Assays

Resting cells assay

For resting cells assays, 50 mL of growth medium were inoculated to an initial OD_{600} of 0.1 in baffled 300 mL flasks. The cultures were incubated at 30°C and 130 rpm for 48 h. Cells were transferred to sterile 50 mL Greiner tubes and centrifuged at 2,500 rpm for 5 min. The supernatant was removed and the cell pellet was resuspended in 50 mL of pre-warmed (30°C) induction medium and transferred to 300 mL baffled flasks. The cultures were incubated at 30°C and 130 rpm for 6 h. Five OD_{600} units were transferred to Eppendorf tubes and stored on ice for Western blot analysis. Two times 300 OD_{600} units were centrifuged in 50 mL Greiner tubes, the supernatants were discarded und the cells were resuspended in 1.4 mL of 50 mM KP_i pH 7.4. Two times 1 mL of resuspended cells were transferred into Pyrex tubes and 20 µL of terpene stock solution were added. Resting cells were incubated at 30°C and 170 rpm over night. Terpenoids were extracted in 500 µL of ethyl acetate by vibraxing for 30 min. Phases were separated by spinnig at 5,000 rpm for 15 min. Seventy µL of ethyl acetate phase were transferred into glass crimp vials with glass inserts for GC-FID measurement.

In vivo assay

For *in vivo* assays, 5 mL of growth medium were inoculated and incubated at 30°C and 170 rpm overnight. Fifty mL of growth medium in 100 mL flasks were inoculated to an initial OD_{600} of 0.1 and incubated at 30°C and 130 rpm for 24 h. Cultures were transferred to a sterile 50 mL Greiner tube and pelleted at 2,500 rpm for 5 min. The supernatant was discarded and the cell pellet was resuspended in 50 mL of pre-warmed (30°C) induction medium. Cells were transferred to 100 mL flasks, overlaid with 5 mL n-hexadecane and incubated at 30°C and 130 rpm for 48 h. Five OD_{600} units were transferred to Eppendorf tubes and stored on ice for Western blot analysis. The two-phase cultivation broth was

transferred to sterile 50 mL Greiner tubes and centrifuged at 2,500 rpm for 5 min. One hundred µL of the upper, organic phase were used for GC-FID measurement.

Resting cells assay: Bufuralol conversion

For bufuralol conversion assays, cells were cultivated as described for resting cells assays. After induction for 6 h in galactose rich media, cells were pelleted and resuspended in 50 mM KP_i pH 7.4. Three times 250 µL were transferred to microfuge tubes, 10 µL of 1 mM bufuralol stock were added and incubated at 30°C, 650 rpm for 30 min. Reaction was stopped by centrifuging at 4°C and full speed for 10 min. Ninetyfive µL supernatant were transferred to 96-deepwell plates, 5 µL of 0.5 mM prednisolone stock was added to a final concentration of 50 ng/µL and the samples were measured with HPLC-MS.

Cell lysis with glass beads

To determine if 1-hydroxybufuralol was retained in the cells, the cells were lysed with glass beads. After 95 µL supernatant was removed for HPLC-MS measurement, glass beads, roughly the same volume as the cell pellet, were added. The cells were lysed by vortexing for 4 min, alternating 30 s vortexing and 30 s cooling on ice. The cell debris and glass beads were spun down at top speed for 5 min. Again, 95 µL supernatant were transferred to 96-deepwell plates, 5 µL of 0.5 mM prednisolone stock was added to a final concentration of 50 ng/µL and the samples were measured with HPLC-MS.

3.11 Western Blot analysis

Riezman cell disruption

For Riezman cell disruption, 5 OD_{600} units of culture were transferred to ice-cold microfuge tubes, centrifuged at 3500 rpm and 4°C for 5 min, and the supernatant was discarded [28]. Pellets were resuspended in 300 µL of resuspension solution, were chilled on ice for 10 min, 300 µL of 50% TCA were added and chilled on ice for 1 h. The mixture was centrifuged at 10,000 rpm and 4°C for 5 min. The supernatant was discarded and the pellet was washed with 500 µL of ice-cold ddH_2O. The pellet was resuspended in 50 µL of sample buffer, denatured at 95°C for 5 min and centrifuged at room temperature for 10 s. Samples were stored at -20°C or immediately loaded onto an SDS-gel.

Western blot analysis

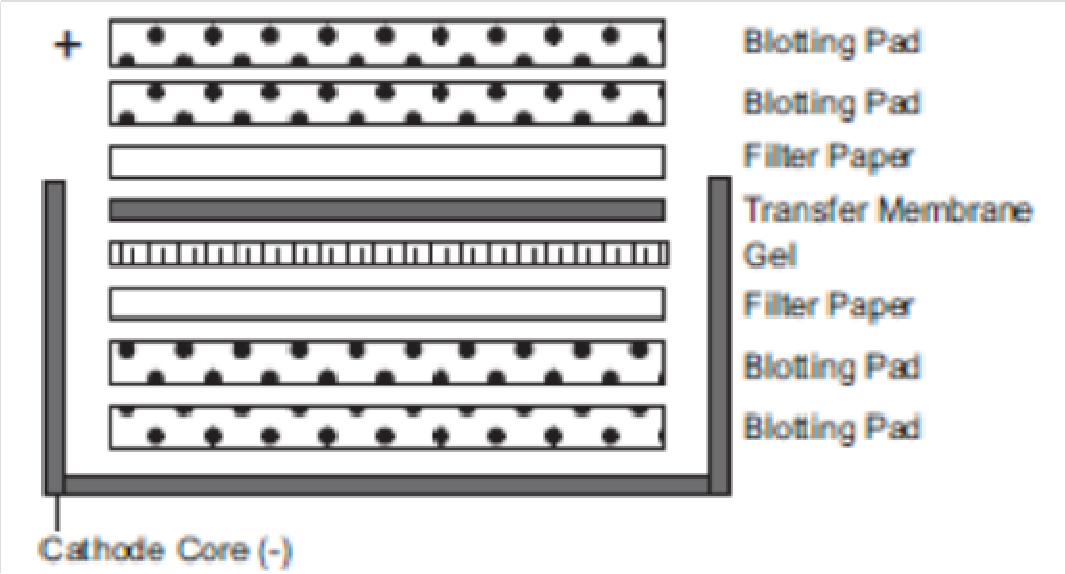

Figure 8: blotting sandwich , source: manual NuPage®

First, 10 µL sample (see Riezmann cell disruption) and 3 µL of protein ladder were loaded onto NuPage® ready-to-use-gels. The gels were run at 30 mA, max V, max W for 1 1/2 h and cut afterwards for use in the blotting sandwich. Blotting pads, filter paper, nitrocellulose transfer membrane and gel were soaked in transfer solution and used to build a blotting sandwich (Figure 8). Formation of air bubbles was avoided. The blotting sandwich was fixed with a Gel Tension Wedge in an X Cell II unit and the blotting was done according to the manual, exposing the sandwich to 250 mA, max V, max W for 1 h.

Nitrocellulose membranes were stained with Ponceau S solution for 10 s to detect transfer efficiency, rinsed with ddH_2O for 10 s and an image was taken. Ponceau S was removed by washing the membranes two times with ddH_2O for 15 min. The membranes were blocked with TBST-milk at room temperature under constant shaking for 1 h, rinsed with TBST and the primary antibodies Anti-c-*myc*-Ab and Anti-FLAG-Ab in TBST-milk were applied at 4°C with shaking overnight. Membranes were washed three times with TBST for 10 min and the secondary antibodies in TBST-milk were applied at room temperature with shaking for 1 h. Again, three washing steps were performed as above. The membrane was covered in 1.5 mL of SuperSignal® West Pico Chemiluminescent Substrate mixture and chemiluminescence was detected with the G-box HR (Syngene, UK) after 2 and 10 min of exposure.

3.12 GC-FID AND HPLC-MS

GC-FID method

Terpenoid extracts were analyzed by GC-FID. Therefore, a HP-5 column (crosslinked 5% Ph-Me Siloxane; 10 m, 0.10 mm in diameter and 0.10 µm film thickness) was used on a Hewlett-Packard 6890 GC equipped with a flame ionization detector (FID). Sample aliquots of 1 µL were injected in split mode at 250°C injector temperature and 320°C detector temperature with H_2 as carrier gas and with a flow rate set to 0.4 mL/min in constant flow mode. The oven temperature program was as follows: 100°C for 1 min, 20°C/min ramp to 250°C and 45°C/min ramp to 280°C (0.5 min). Total run time was 21 min. The program running the analysis and recording the data was Instrument #1 Data Analysis, MSD ChemStation D.03.00552, Agilent Technologies. The program used to determine the concentrations was Agilent ChemStation B.0302, Agilent Technologies.

HPLC-MS method

Samples of bufuralol conversion assays were analyzed by HPLC-MS. Metabolites were separated on a XDB-C18 column using 10 mM ammonium acetate, pH 5.0, and acetonitrile (ACN) as mobile phase. A gradient was applied to separate bufuralol, 1-hydroxybufuralol and prednisolone: 0-1.6 min, 20% ACN; 1.61-3.0 min, 40% ACN; 3.01-4.0 min, 20% ACN. Concentrations of bufuralol and 1-hydroxybufuralol were quantified by an external calibration using the reference metabolite prednisolone.

3.13 CO-DIFFERENCE SPECTROSCOPY

Isolation of total microsomes

Five mL growth medium in 50 mL Greiner tubes were inoculated and incubated at 30°C and 170 rpm overnight. Fifty mL growth medium in baffled 300 mL flasks were inoculated with an ONC to an initial OD_{600} of 0.1 and incubated at 30°C and 130 rpm for 24 h. Cells from the second ONC were used to inoculate 200 mL of growth medium in baffled 2 L flasks to an OD_{600} of 0.1. Main cultures were incubated at 30°C and 130 rpm for 48 h. For induction, cells were centrifuged in JA-10 centrifuge vessels at 2,500 rpm for 5 min, resuspended in 200 mL of induction medium and incubated at 30°C and 130 rpm for 6 h.

To isolate total microsomes, cells were centrifuged in JA-10 centrifuge vessels at 5,000 rpm and 4°C for 5 min, washed with deionized water and centrifuged again. Cell wet weight (CWW) was determined, the cell pellet was resuspended in TE-buffer and 2 µL of 1 m PMSF per g CWW added. Resuspended cells were transferred to Merckenschlager vessels, which were filled to one third with glass beads and one third with cell suspension. Merckenschlager vessels were placed in the Merckenschlager device and pre-cooled with CO_2 for 15 s. Cell disruption was done for 3 min with CO_2 cooling every 30 s. Cell lysates were transferred into JA-25.50 centrifuge vessels and spun at 5,000 rpm and 4°C for 10 min. The supernatants were twice centrifuged at 10,000 rpm and 4°C for 15 min. The final supernatants were transferred to ultracentrifuge vessels for rotor Ti 70 to be centrifuged at 45,000 rpm and 4°C for 45 min. Total microsomal fractions were resuspended in Tris buffer pH 7.4 and stored at -80°C.

Measurement of CO-difference spectra

To measure the CO-difference spectra, 200 µL of isolated microsomes were transferred to 96 well plates and 10 µL of 200mM KCN solution and a small amount of sodium dithionite were added. The plate was shaken for 1 min and the baseline was recorded with the plate reader (POLARstar Galaxy, BMG Labtech GmbH). Next, the plate was fumigated with CO for 3 min. Finally, the CO-difference spectrum was recorded in the range of 380 to 510 nm.

4. RESULTS

4.1 CLONING

Cloning of pESC URA3 P_{GAL1}-hCPR-myc P_{GAL1}-CYP2D6-Flag

For generating of co-expression plasmid pESC *URA3* hCPR opt. CYP2D6 opt., the vector pESC *URA3* and synthetic gene hCPR were restricted with *EcoR*I and *Not*I overnight. Vector backbone and hCPR were run on a gel and purified (Figure 9).

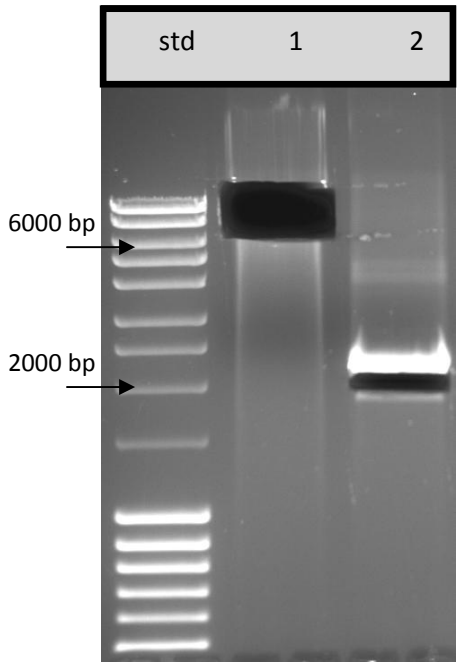

ID	Fragment	~ Size [bp]
1	pESC URA3	6500
2	hCPR-*myc*	2000

Figure 9: Preparative gel of digested pESC *URA3* and hCPR-myc, standard= MassRuler™ DNA Ladder Mix (Thermo Scientific, USA)

DNA concentrations were determined by NanoDrop. The concentration for pESC *URA3* was 76.5 ng/µL and for hCPR-myc 14.1 ng/µL. pESC *URA3* P_{GAL1}-hCPR-*myc* ligation constructs were tested positive via restriction analysis with *EcoR*I and *Not*I (Figure 10).

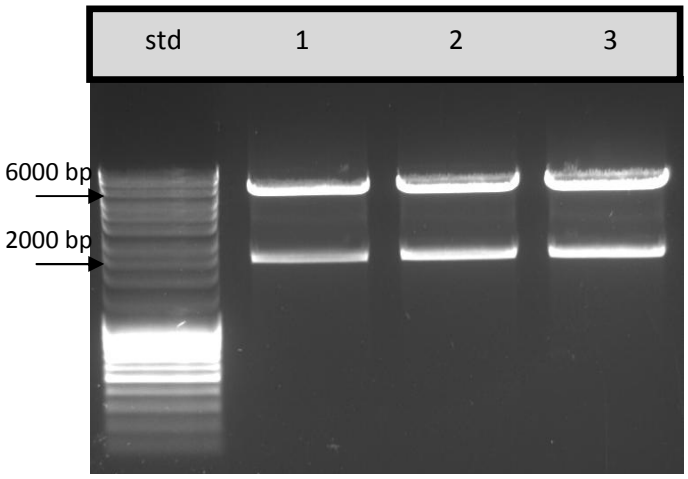

ID	Plasmid	~ Size [bp]
1	pESC URA3 P_{GAL1}-hCPR-*myc*	6500, 2000
2	pESC URA3 P_{GAL1}-hCPR-*myc*	6500, 2000
3	pESC URA3 P_{GAL1}-hCPR-*myc*	6500, 2000

Figure 10: Control gel of pESC URA3 PGAL1-hCPR-myc cut with NotI and EcoRI, standard = MassRuler™ DNA Ladder Mix (Thermo Scientific, USA)

Plasmid pESC URA3 P_{GAL1}-hCPR-*myc* and synthetic gene CYP2D6-Flag were cut with *Hind*III, gel-purified and were separately cut with *BamH*I. Next, a standard preparative gel was run for fragment purification (Figure 11).

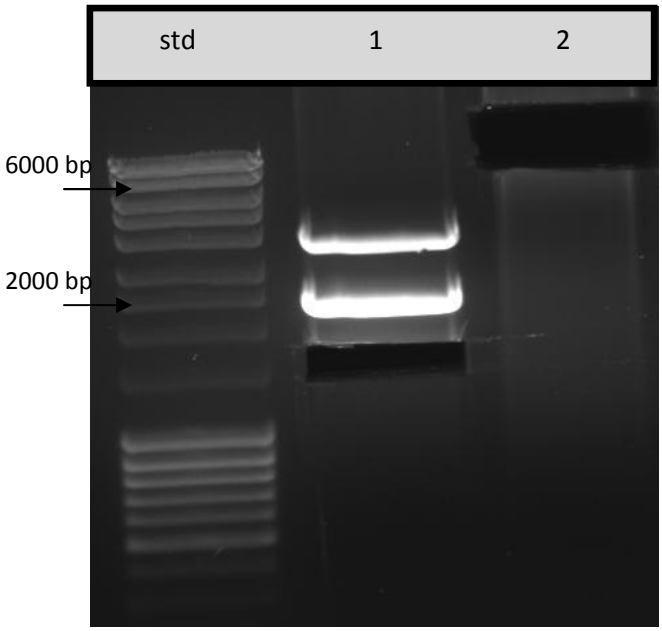

ID	Fragment	~ Size [bp]
1	CYP2D6-FLAG	1500
2	pESC URA3 P_{GAL1}-hCPR-*myc*	8500

Figure 11: Preparative gel of pESC URA3 P_{GAL1}-hCPR-*myc* and CYP2D6-Flag, standard = MassRuler™ DNA Ladder Mix (Thermo Scientific, USA)

After fragment isolation and clean-up, concentrations of the DNA fragments were determined by NanoDrop. The concentration for pESC *URA3* P_{GAL1}-hCPR-*myc* was 80.9 ng/µL and for CYP2D6-Flag 17.6 ng/µL. Vector and insert were ligated as described in the Methods section. Control cuts were performed with *Eco*RI, *Not*I and *BamH*I, *Not*I to verify correct

cloning of pESC URA3 P_{GAL1}-hCPR-*myc* P_{GAL1}-CYP2D6-Flag vector (Figure 12). The vector map of the final construct is shown in Figure 13.

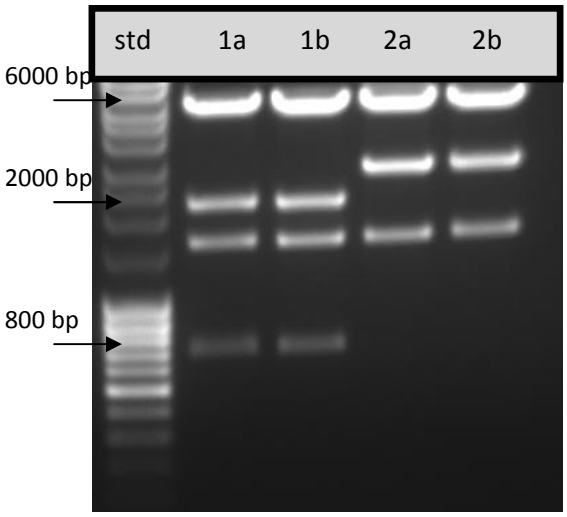

ID	Restriction enzymes	~ Size [bp]
1a	*EcoR*I, *Not*I	5950, 2100 1600, 700
1b	*EcoR*I, *Not*I	5950, 2100 1600, 700
2a	*BamH*I, *Not*I	5950, 2800 2100
2b	*BamH*I, *Not*I	5950, 2800 2100

Figure 12: Control cuts of pESC URA3 PGAL1-hCPR-myc PGAL1-CYP2D6-Flag, standard = MassRuler™ DNA Ladder Mix (Thermo Scientific, USA)

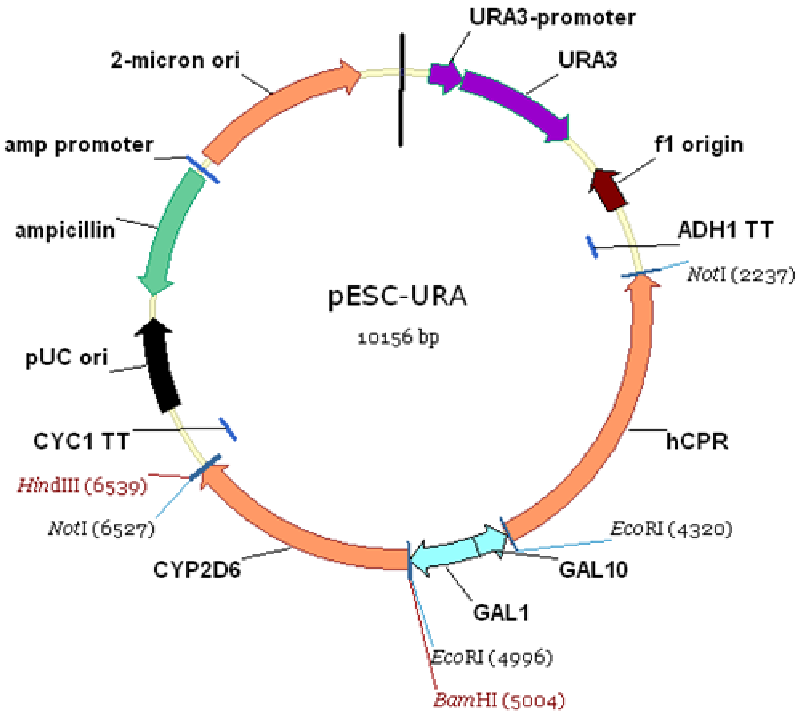

Figure 13: pESC URA P_{GAL1}-hCPR-*myc* P_{GAL1}-CYP2D6-Flag

4.2 *S. CEREVISIAE* STRAIN CONSTRUCTION

TRANSFORMATION OF EXPRESSION CASSETTES

Genes of interest were inducible expressed by inserting the *GAL1*-promoter upstream into the genome (Figure 14).

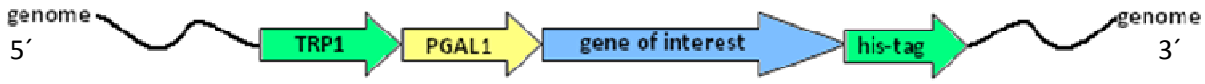

Figure 14: Cloning strategy for expressing endogenous genes from P_{GAL1}

Cloning of W303 *MATα ice2*::P_{GAL1}-*ICE2*His_6

Cassette *TRP*1-P_{GAL1}-*ICE2*His_6 was amplified via PCR using primers F1(*ICE2*_350) and R1(*ICE2*) and the template pFA6a-*TRP*1 P_{GAL1}-*ICE2*His_6. Afterwards, a standard preparative gel was run for fragment purification (Figure 15).

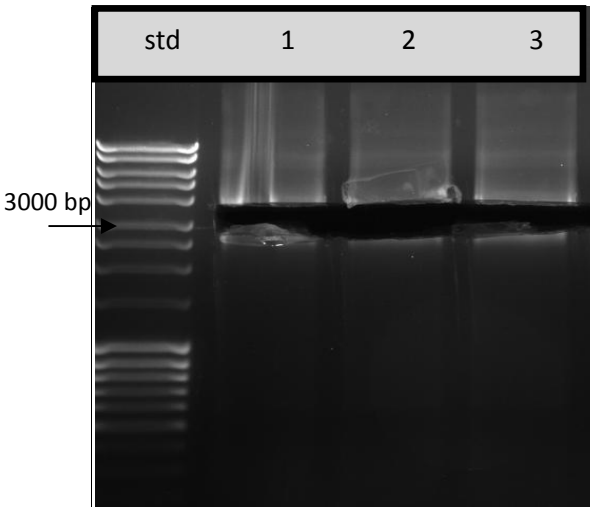

Figure 15: Preparative gel of overexpression cassettes *TRP1*-P_{GAL1}-*ICE2*His6, standard = MassRuler™ DNA Ladder Mix (Thermo Scientific, USA)

W303 *MATα* cells were transformed with the isolated cassette following the protocol for lithium acetate transformation. Transformants were selected on SD-trp plates at 30°C. A cPCR was performed identifying positive transformants using primers Fw(start *GAL1*) and Rv(*ICE2*) (Figure 16). Positive integration of P_{GAL1} in front of the gene resulted in a PCR fragment of ~ 750 bp.

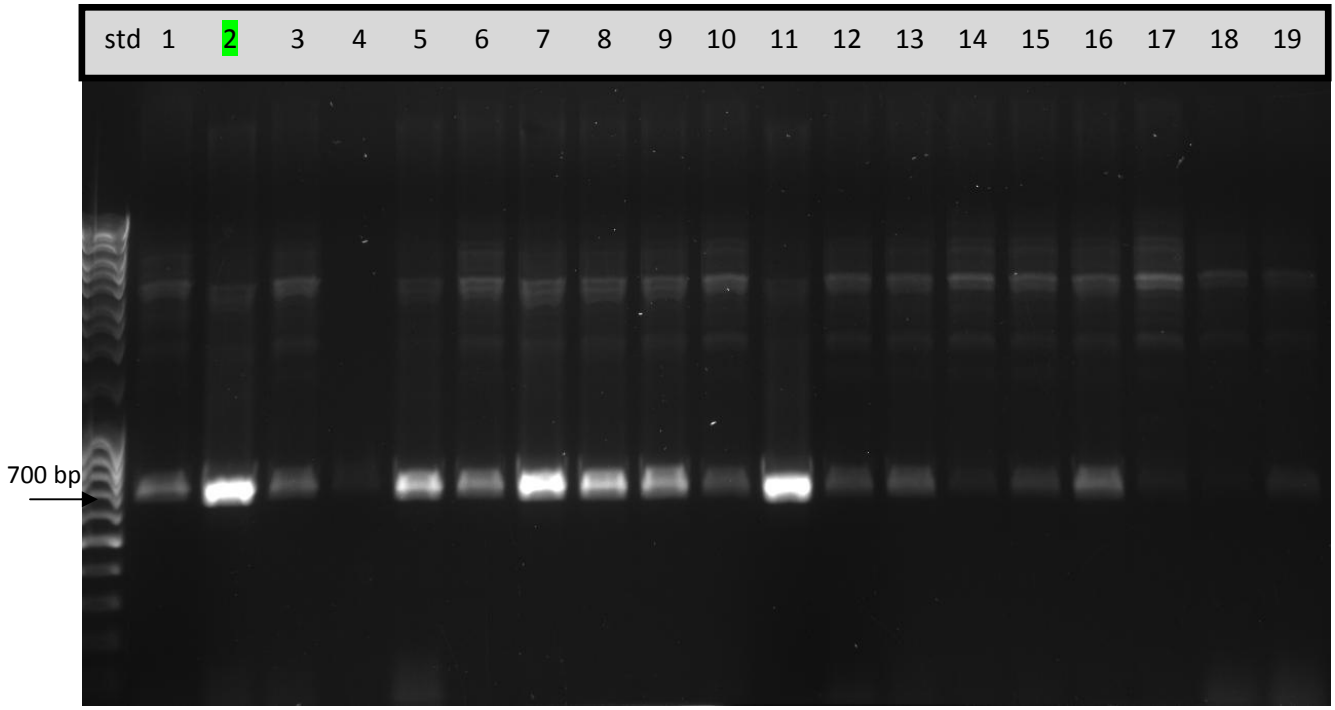

Figure 16: Colony PCR of strain W303 *MATα ice2*::P_{GAL1}-*ICE2*His_6, standard = MassRuler™ DNA Ladder Mix (Thermo Scientific, USA), number 1-19 each represents a tested strain

Each band at 750 bp represents a positively tested strain. Strain number 2 was selected for testing in assays.

TRANSFORMATION OF PLASMIDS

Plasmids were amplified in *E. coli* Top 10 F´ cells for transformation of *S. cerevisiae*. An example of a positively transformed strain is displayed in Figure 17.

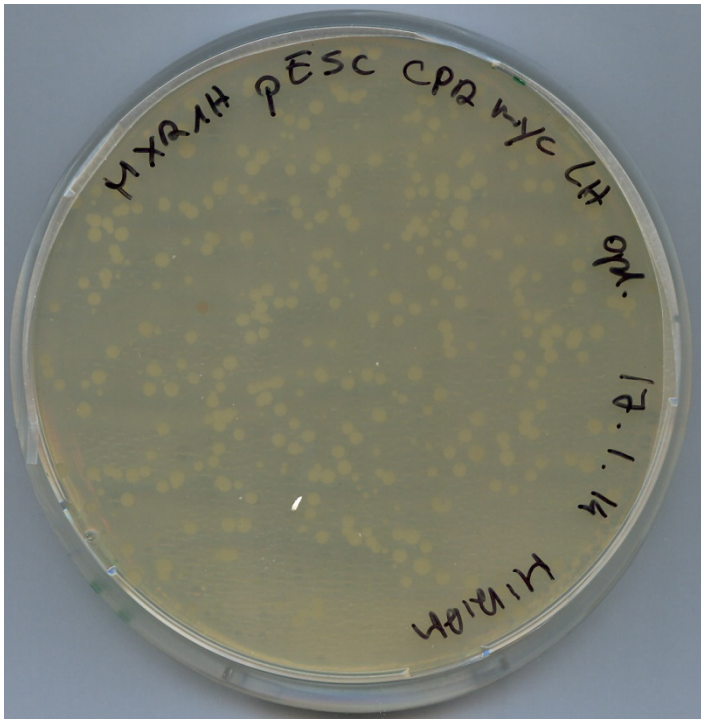

Figure 17: Example for transformants after lithium acetate transformation. W303 *MATα* P_{GAL1}-*MXR1*His6 was transformed with pESC *URA3* P_{GAL1}-CPR-*myc* P_{GAL1}-PM17-Flag

Table 10: List of strains containing plasmids

Strain	Plasmid
S. cerevisiae W303 *MATa*	pYES2 P_{GAL1}-CPR-*myc* P_{GAL1}-HPO-Flag
S. cerevisiae W303 *MATα* his3::P_{GAL1}-*ICE2*His_6	pYES2 P_{GAL1}-CPR-*myc* P_{GAL1}-HPO-Flag
S. cerevisiae W303 *MATa*	pRS413 P_{GPD}-LimS opt.
S. cerevisiae W303 *MATa* leu2::P_{PGK}-t*HMG*1	pRS413 P_{GPD}-LimS opt.
S. cerevisiae W303 *MATa*	pRS413 P_{GPD}-LimS opt. pESC URA P_{GAL1}-CPR-*myc* P_{GAL1}-PM17 opt.-Flag
S. cerevisiae W303 *MATa* leu2::P_{PGK}-t*HMG1*	pRS413 P_{GPD}-LimS opt. pESC URA P_{GAL1}-CPR-*myc* P_{GAL1}-PM17 opt.-Flag
S. cerevisiae W303 *MATα*	pESC URA P_{GAL1}-CPR-*myc* P_{GAL1}-PM17 opt.-Flag
S. cerevisiae W303 *MATα* P_{GAL1}-*DAP1*	pESC URA P_{GAL1}-CPR-*myc* P_{GAL1}-PM17 opt.-Flag
S. cerevisiae W303 *MATα* P_{GAL1}-*ICE2*	pESC URA P_{GAL1}-CPR-*myc* P_{GAL1}-PM17 opt.-Flag
S. cerevisiae W303 *MATα* P_{GAL1}-*SUR1*	pESC URA P_{GAL1}-CPR-*myc* P_{GAL1}-PM17 opt.-Flag
S. cerevisiae W303 *MATα* his3::P_{GAL1}-I*CE2*His_6	pESC URA P_{GAL1}-CPR-*myc* P_{GAL1}-PM17 opt.-Flag
S. cerevisiae W303 *MATα* P_{GAL1}-*KAR2*His_6	pESC URA P_{GAL1}-CPR-*myc* P_{GAL1}-PM17 opt.-Flag
S. cerevisiae W303 *MATα* P_{GAL1}-*LHS1H*is_6	pESC URA P_{GAL1}-CPR-*myc* P_{GAL1}-PM17 opt.-Flag
S. cerevisiae W303 *MATα* P_{GAL1}-*MXR1*His_6	pESC URA P_{GAL1}-CPR-*myc* P_{GAL1}-PM17 opt.-Flag
S. cerevisiae W303 *MATα* P_{GAL1}-*RAD52*His_6	pESC URA P_{GAL1}-CPR-*myc* P_{GAL1}-PM17 opt.-Flag
S. cerevisiae W303 *MATα*	pESC URA P_{GAL1}-hCPR –*myc* P_{GAL1}-CYP2D6-Flag
S. cerevisiae W303 *MATα* P_{GAL1}-*ICE2His*$_6$	pESC URA P_{GAL1}-hCPR –*myc* P_{GAL1}-CYP2D6-Flag
S. cerevisiae W303 *MATα* P_{GAL1}-*LHS1H*is_6	pESC URA P_{GAL1}-hCPR –*myc* P_{GAL1}-CYP2D6-Flag
S. cerevisiae W303 *MATα* P_{GAL1}-*KA*R2His_6	pESC URA P_{GAL1}-hCPR –*myc* P_{GAL1}-CYP2D6-Flag
S. cerevisiae W303 *MATα* P_{GAL1}-*RAD52*His_6	pESC URA P_{GAL1}-hCPR –*myc* P_{GAL1}-CYP2D6-Flag

4.3 VALENCENE CONVERSION ASSAY

Fully functional membrane proteins are difficult to isolate and to apply for conversion assays. Therefore, Anita Emmerstorfer established an assay using whole-cellular systems [14]. A major drawback of using whole cells is the limitation of substrate availability due to phase transfer issues. However, the P450 enzymes could operate in native cell environments being naturally supplied with cofactors and protected against shear forces, which would not be the case, if cell lysates were used.

After growth and induction phases, cells were centrifuged and resuspended in buffer to be used as resting cells (chapter 0). (+)-Valencene is hardly soluble in aqueous milieus, hence it was added to resting cells as a 100 mM stock in DMSO. Also, 1 % Triton™ X-100 was added to improve transport of substrate and products. After 16 h of conversion, terpenoids were extracted with ethyl acetate. This solvent did neither interfere with peak identification in GC-FID itself, nor did it extract any other substances that did. Substrate and products were highly volatile in aqueous environment, which posed a problem for the performance of the assays. The substrate stock solution had to be added quickly to keep the loss due to evaporation low. All steps after substrate addition had to be performed reproducibly to keep terpenoid loss and the results comparable.

Quantification of terpenoids

To quantify the substrates and products of the (+)-valencene conversion assay, calibration curves of (+)-valencene, cis-nootkatol, trans-nootkatol and (+)-nootkatone concentrations in ethyl acetate were created with the help of Prof. Erich Leitner, Institute of Analytical Chemistry and Food Chemistry of Graz University of Technology [14].

An example of the analysis of an ethyl acetate extract is shown in Figure 18.

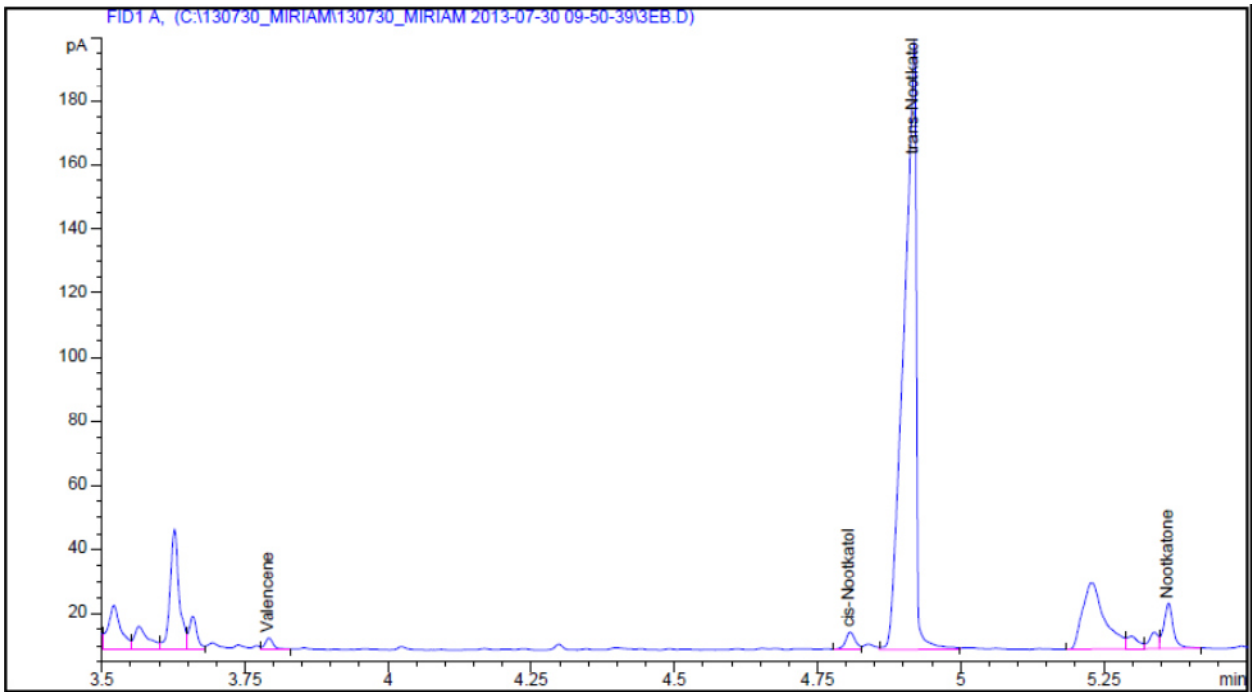

RetTime [min]	Type	Area [pA*s]	Amt/Area	Amount [ng/ul]	Grp	Name
3.792	VV	3.59013	6.87457e-1	2.46806		Valencene
4.807	VV	6.32823	1.06795	6.75826		cis-Nootkatol
4.919	VV	284.87723	2.34913	669.21421		trans-Nootkatol
5.363	VB	16.08170	1.01352	16.29905		Nootkatone
Totals :				694.73957		

Figure 18: Chromatogram of one of the samples shown in Figure 19, the sample contains different amounts of (+)-valencene, cis-nootkatol, trans-nootkatol and (+)-nootkatone measured with GC-FID

Effect of alternative carbon sources and induced expression of *ICE2* on (+)-valencene conversion

The effect of adding ethanol or glycerol as alternative carbon sources was tested in (+)-valencene conversion assays. Usually, cell cultures had been incubated at 30°C for 48 h before inducing the cells (chapter 0). Here, cells were cultured with an initial glucose concentration of only 1 % and 2 % of alternative carbon sources were added after 24 h of growth. Cells were further incubated for 24 h. Resting cells assays were set up as described in the Methods section.

Table 11: Strains tested in (+)-valencene conversion assay

ID	Strain
Pos	W303 *MATα* pYES2 P_{GAL1}-CPR-*myc* P_{GAL1}-HPO-Flag
ICE2	W303 *MATα* P_{GAL1}-*I*CE2 pYES2 P_{GAL1}-CPR-*myc* P_{GAL1}-HPO-Flag

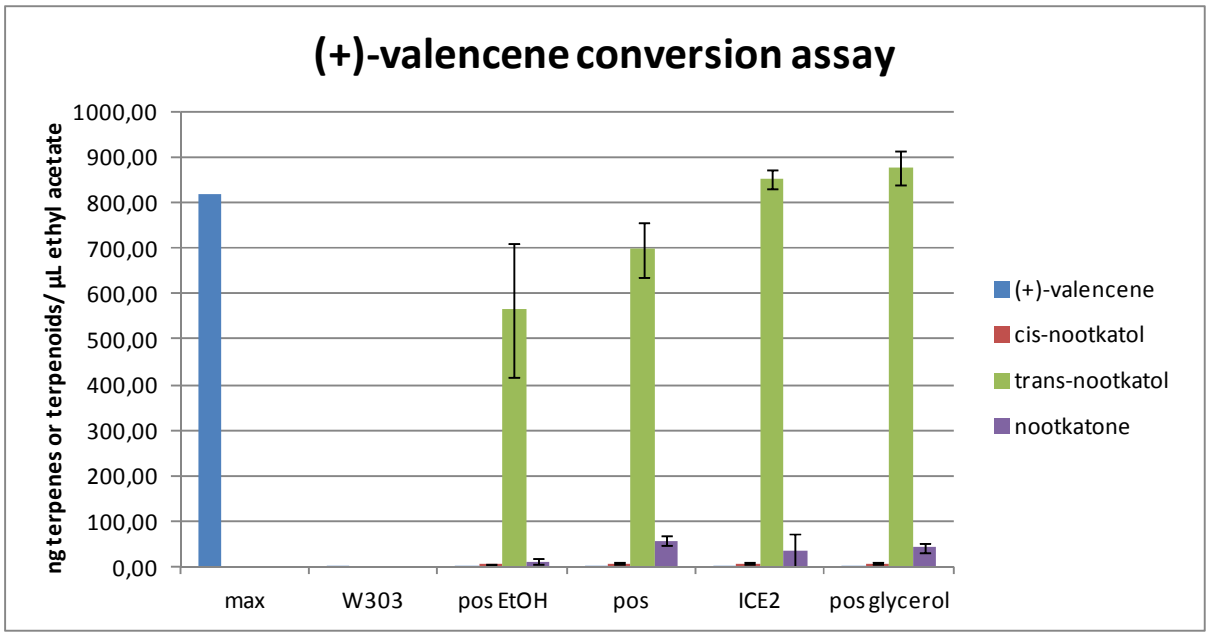

Figure 19: (+)-Valencene conversion assay, max represents the initial (+)-valencene concentration, strains listed in Table 11 were tested, 2 biological and 4 technical replicates were tested per sample , data represented as means and standard deviation

The addition of glycerol as alternative carbon source during the growth phase did improve conversion to the same extent, as expression of *ICE2* from P_{GAL1} did (Figure 19). The addition of ethanol insignificantly lowered conversion rates. Anita Emmerstorfer tested P_{GAL1} driven expression of *ICE2* in (+)-valencene *in vivo* synthesis and found it to have a beneficial effect [14].

4.4 LIMONENE *IN VIVO* SYNTHESIS AND CONVERSION

4.4.1. PRODUCTION AND PURIFICATION OF ISOPIPERITENOL

Isopiperitenol is not available as a standard and is also difficult to make chemically. Therefore, we produced isopiperitenol during a (-)-limonene resting cells assay using strain W303 *MATα* pESC URA P_{GAL1}-CPR-*myc* P_{GAL1}-PM17 opt.-Flag. Resting cells assays with cells resulting from 1 L of yeast culture were performed as described in methods (chapter 0). After the extraction with ethyl acetate, the entire organic phases were combined and isopiperitenol was purified by Gernot Strohmeier, Institute of Organic Chemistry, Graz University of Technology.

For the purification of isopiperitenol, a flash column chromatography was performed on Merck silica gel 60 (0.040-0.063 mm, 60 Å). The volatiles of the ethyl acetate extract were evaporated and the residue (49 mg) was purified by flash column chromatography (3 g silica gel, 6 × 1 cm, cyclohexane/ethyl acetate = 25:1). All fractions containing the product (R_f = 0.37, cyclohexane/ethyl acetate 4:1; phosphomolybdic acid staining; 60-100 mL elution volume) were pooled and evaporated under reduced pressure. The yield of the purification was 4.8 mg isopiperitenol. A GC-MS analysis confirmed that our co-expression system produced isopiperitenol (Figure 20).

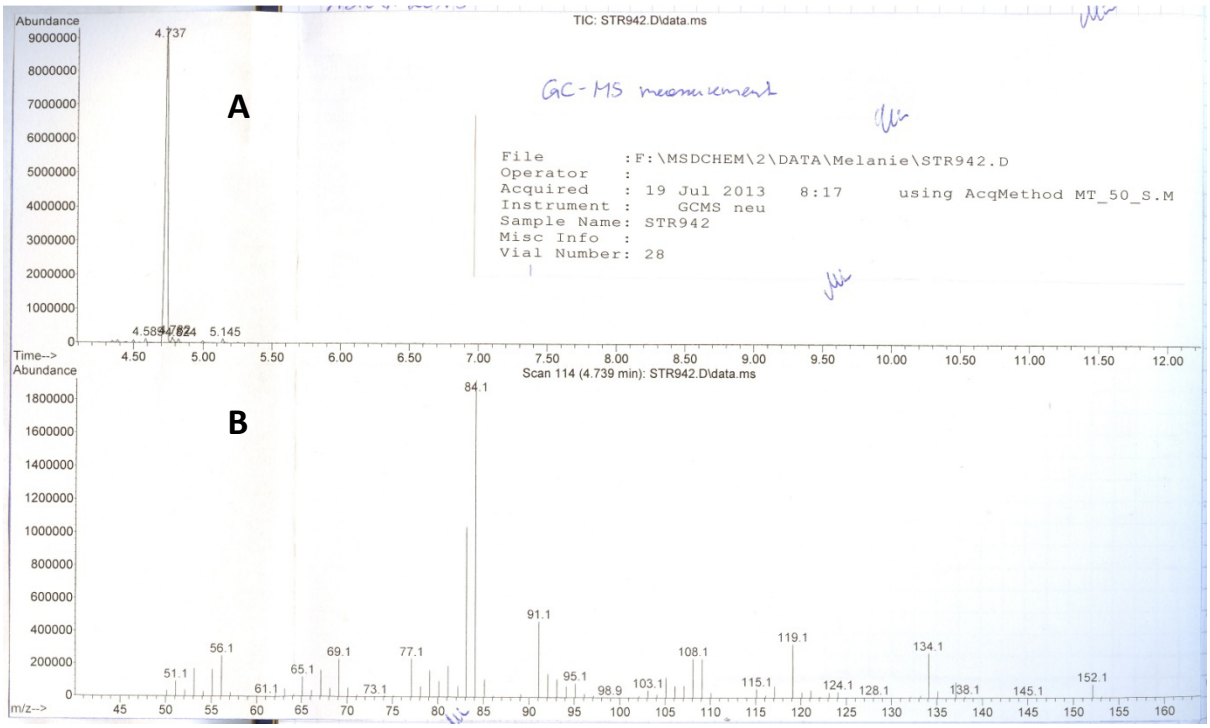

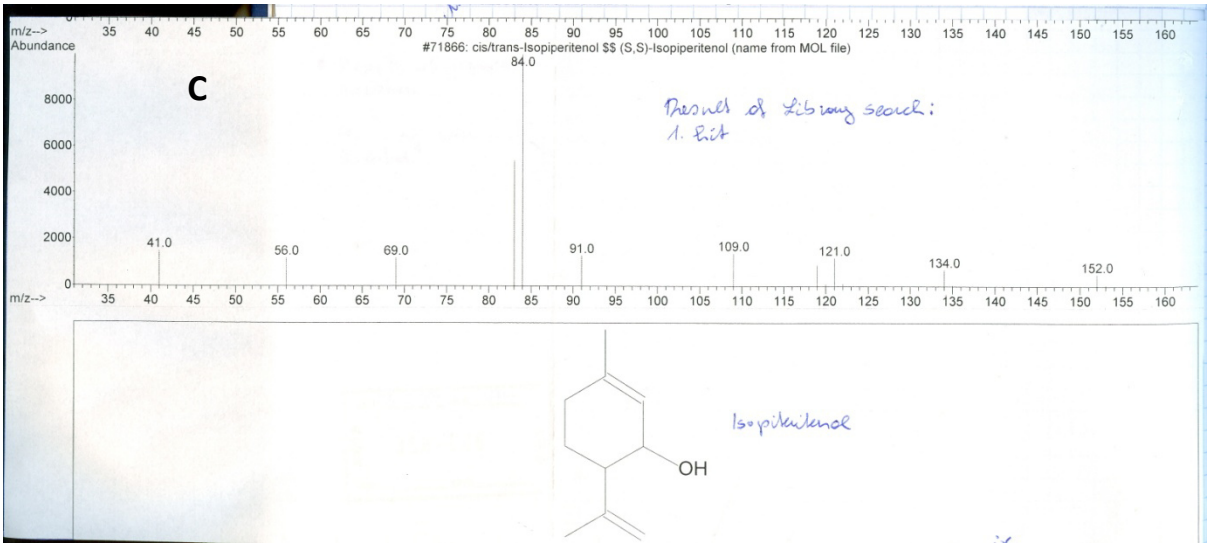

Figure 20: Results of the GC-MS analysis of isopiperitenol; A: GC analysis, B: results of MS analysis of isopiperitenol, C: MS spectrum of isopiperitenol out of MS-library (Agilent Technologies)

4.4.2. LIMONENE IN VIVO SYNTHESIS

Earlier in this project, Anita Emmerstorfer had established an *in vivo* (+)-valencene synthesis assay [14], (chapter 0). n-Dodecane was used to trap the volatile (+)-valencene which is insoluble in aqueous culture media. However, n-dodecane could not be used in (-)-limonene conversion assays because the solvent peak interferred with the (-)-limonene peak. Therefore, n-hexadecane was used as second, organic layer. However, (-)-limonene was detected in the n-hexadecane phase. Different explanations can be given: Either, limonene synthase was not expressed to high levels or inactive form for product formation or (-)-limonene simply could not be efficiently entrapped in the n-hexadecane phase. To test, whether a phase transfer or (-)-limonene toxicity issue was the reason, strains which could both synthesise and directly convert (-)-limonene to the less volatile isopiperitenol were tested for *in vivo* (-)-limonene synthesis and conversion (Table 12). Therefore, strains containing vector pRS413 P_{GPD}-LimS opt. were inserted with vector pESC *URA3* P_{GAL1}-CPR-*myc* P_{GAL1}-PM17 opt.-Flag too. Thus, these strains were enabled to perform both (-)-limonene *in vivo* synthesis and conversion.

Table 12: Strains tested in (-)-limonene synthesis and conversion assay

ID	strain
pos	W303 *MATα* pRS413 P_{GPD}-LimS opt.
t*HMG1* LimS	W303 *MATα* P_{PGK1}-tHMG1 pRS413 P_{GPD}-LimS opt.
LimS PM17	W303 *MATα* pRS413 P_{GPD}-LimS opt. pESC URA P_{GAL1}-CPR-*myc* P_{GAL1}-PM17 opt.-Flag
t*HMG1* LimS PM17	W303 *MATα* P_{PGK1}-tHMG1 pRS413 P_{GPD}-LimS opt. pESC URA P_{GAL1}-CPR-*myc* P_{GAL1}-PM17 opt.-Flag
neg	W303 *MATα* . pESC URA P_{GAL1}-CPR-*myc* P_{GAL1}-PM17 opt.-Flag

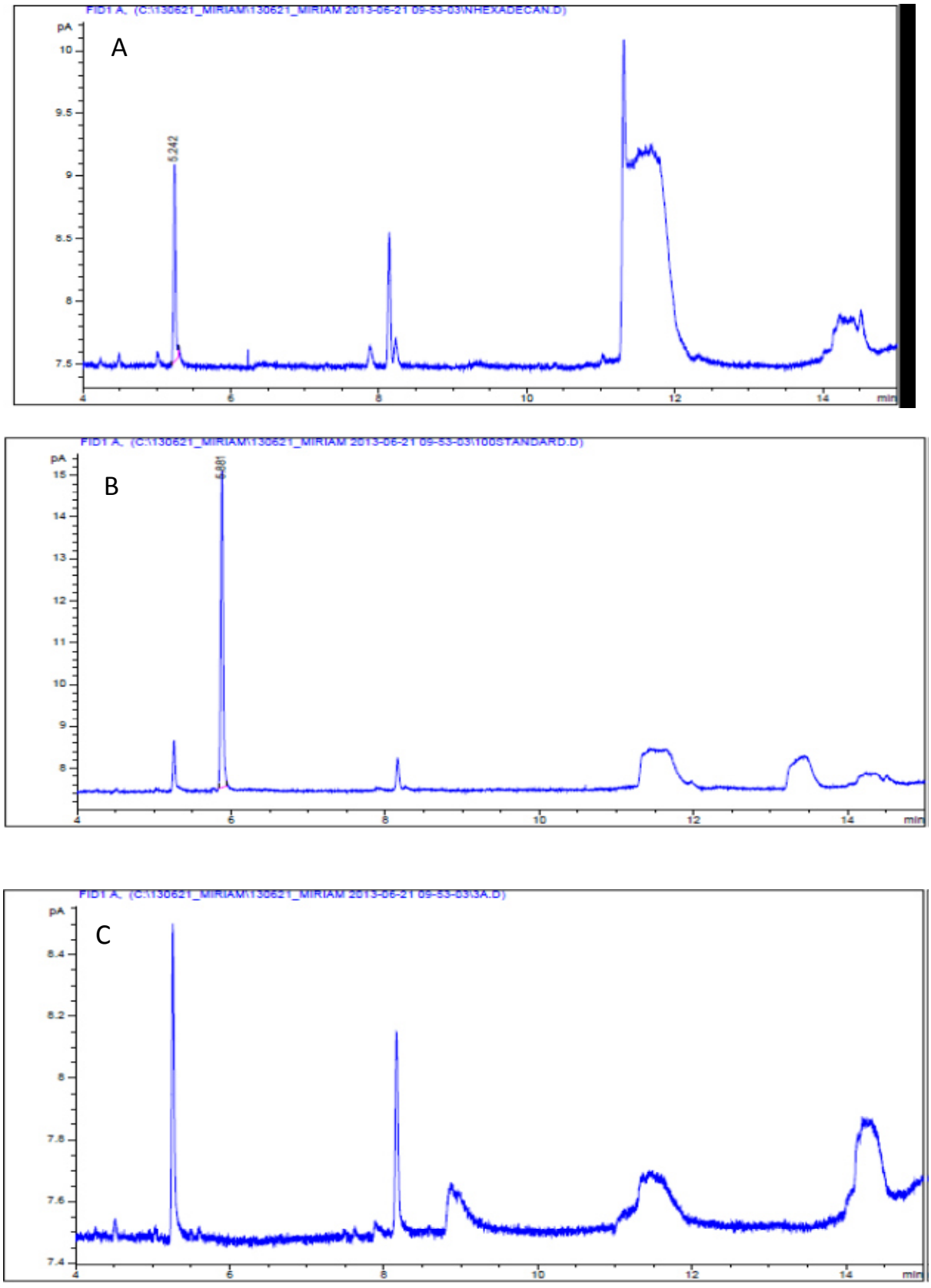

Figure 20: Chromatograms of (-)-limonene synthesis and conversion assay; A n-hexadecane, B (-)-limonene and isopiperitenol standard, C strain LimS PM17

The strains produced no detectable amounts of (-)-limonene or isopiperitenol (Figure 21). Concomitantly, strains were analyzed by Western blot for expression of (-)-limonene synthase. The size of LimS is approximately 60 kDa.

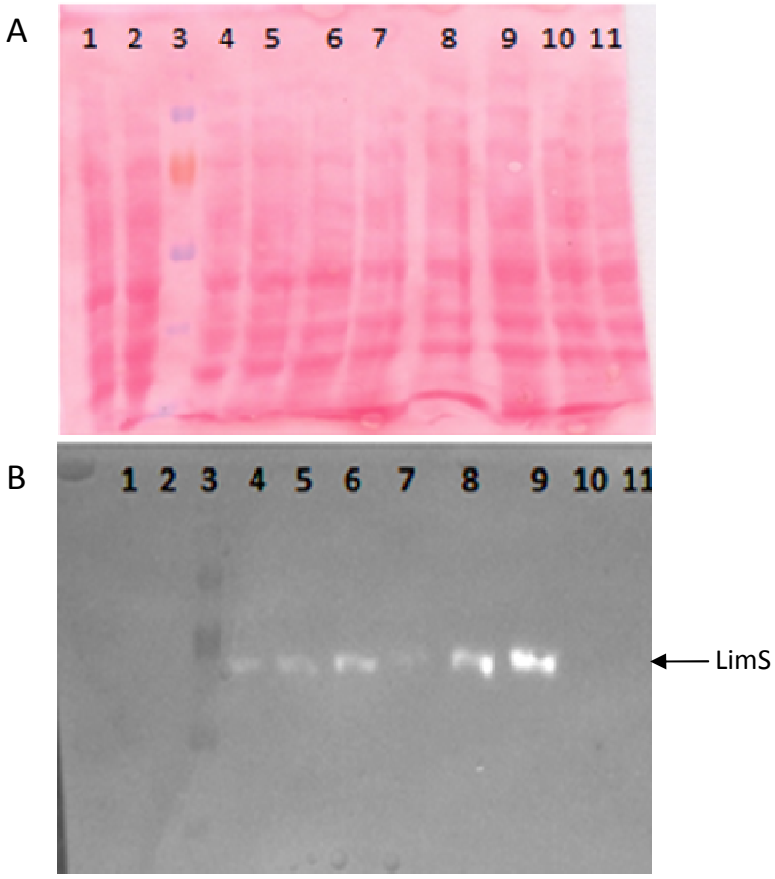

Figure 21: Western blot analysis of samples from limonene synthesis and conversion assay, A = Ponceau S staining, B = chemiluminescence image, samples are described in Table 12

Table 13: Samples tested via Western blot analysis (Figure 22)

ID	sample
1	W303 *MATa* pRS413 P_{GPD}-LimS opt.
2	W303 *MATa* pRS413 P_{GPD}-LimS opt.
3	Page Ruler™ Prestained Ladder, ThermoScientific
4	W303 *MATa* leu::P_{PGK} t*HMG1* pRS413 P_{GPD}-LimS opt.
5	W303 *MATa* leu::P_{PGK} t*HMG1* pRS413 P_{GPD}-LimS opt.
6	W303 *MATa* pRS413 P_{GPD}-LimS opt. pESC URA P_{GAL1}-CPR-*myc* P_{GAL1}-PM17 opt.-Flag
7	W303 *MATa* pRS413 P_{GPD}-LimS opt. pESC URA P_{GAL1}-CPR-*myc* P_{GAL1}-PM17 opt.-Flag
8	W303 *MATa* leu::P_{PGK} t*HMG1* pRS413 P_{GPD}-LimS opt. pESC URA P_{GAL1}-CPR-*myc* P_{GAL1}-PM17 opt.-Flag
9	W303 *MATa* leu::P_{PGK} tHMG1 pRS413 P_{GPD}-LimS opt. pESC URA P_{GAL1}-CPR-*myc* P_{GAL1}-PM17 opt.-Flag
10	W303 *MATα* pESC URA P_{GAL1}-CPR-*myc* P_{GAL1}-PM17 opt.-Flag (negative control)
11	W303 *MATα* pESC URA P_{GAL1}-CPR-*myc* P_{GAL1}-PM17 opt.-Flag (negative control)

(-)-Limonene synthase was expressed in strains coexpressing t*HMG1* or PM17/CPR opt. (Figure 22). This result suggested that the (-)-limonene sythase was either not functional or the overall activity was too low. Another problem might be the catalytic mechanism of FPPS.

4.4.3. LIMONENE CONVERSION

Quantification of terpenes and terpenoids

To quantify the substrates and products of the (-)-limonene conversion assay, calibration curves of (-)-limonene, isopiperitenol and isopiperitenon in ethyl acetate for GC-MS were established. Three different concentration were analysed for each substance. With the calibration curves' linear equations the concentrations in each sample were calculated (Figure 23).

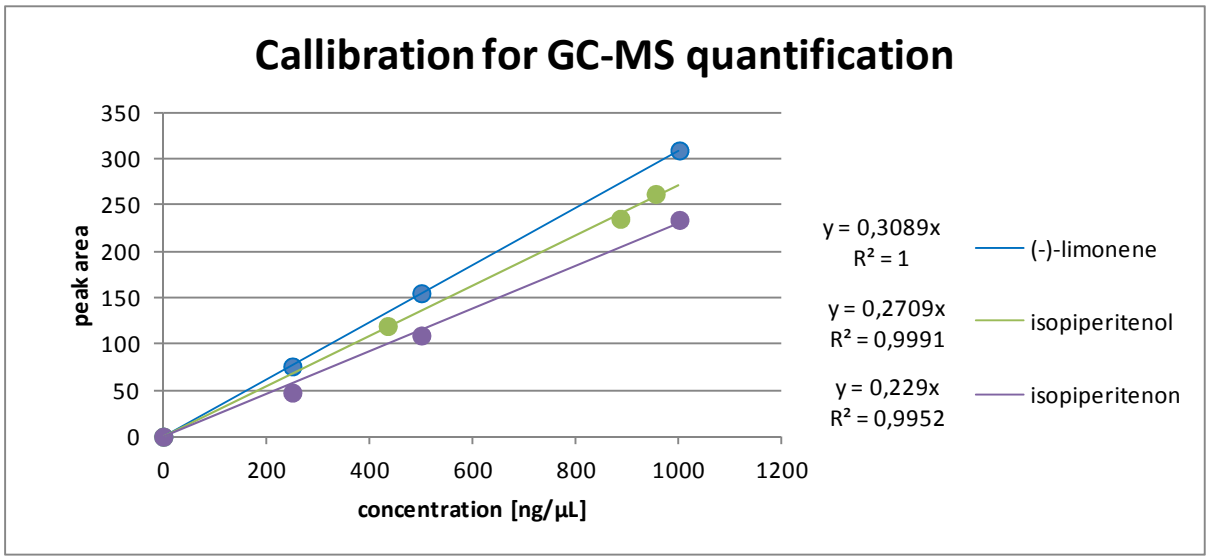

Figure 22: Calibration curves

An example for a chromatogram of (-)-limonene and isopiperitenon standards measured by GC-FID is depicted in Figure 24.

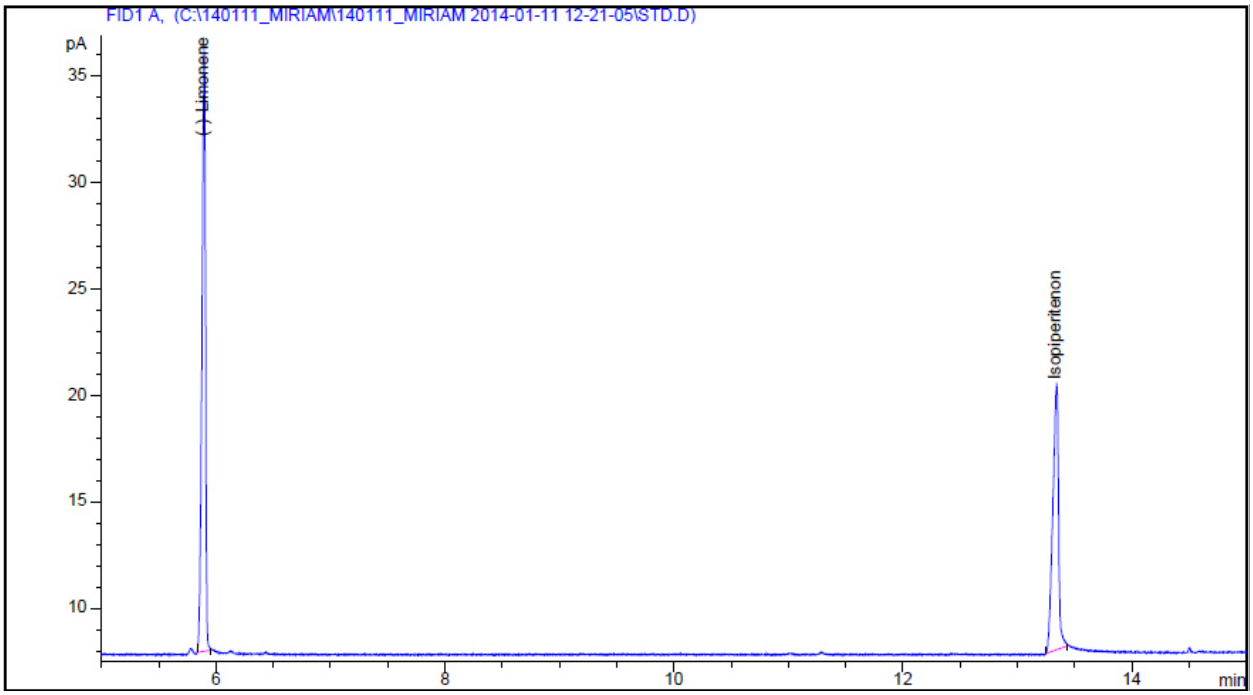

RetTime [min]	Type	Area [pA*s]	Amt/Area	Amount [ng/ul]	Grp	Name
5.899	BB	60.73495	3.25932	197.95451		(-)-Limonene
11.383		-	-	-		Isopiperitenol
13.343	BB	43.35025	4.80008	208.08481		Isopiperitenon
Totals :				406.03933		

Figure 23: Chromatogram of standards measured with GC-FID

Conversion with different initial concentrations

Previously, overexpression of *DAP1*, *I*CE2 and *SUR*1 from the P_{GAL1}-promoter had shown to improve conversion of (+)-valencene in resting cells assays [14], [30]. Therefore, these strains were transformed with co-expression plasmid pESC URA P_{GAL1}-CPR-*myc* P_{GAL1}-PM17 opt.-Flag to be tested for their effect on (-)-limonene conversion in resting cells assay (Table 14).

Table 14: Strains used for (-)-limonene conversion assay with different initial concentrations

ID	strain
W303, neg	W303 *MATα*
Pos	W303 *MATα* pESC URA P_{GAL1}-CPR-*myc* P_{GAL1}-PM17 opt.-Flag
DAP1	W303 *MATα* P_{GAL1}-*DA*P1 pESC URA P_{GAL1}-CPR-*myc* P_{GAL1}-PM17 opt.-Flag
ICE2	W303 *MATα* P_{GAL1}-*IC*E2 pESC URA P_{GAL1}-CPR-*myc* P_{GAL1}-PM17 opt.-Flag
SUR2	W303 *MATα* P_{GAL1}-*SU*R1 pESC URA P_{GAL1}-CPR-*myc* P_{GAL1}-PM17 opt.-Flag

As established for (+)-valencene resting cells assays, 20 µL of 100 mM (-)-limonene stock solution were added to 1 mL of resting cells resuspended in 50 mM KP_i, pH 7.4, to reach an initial concentration of 2 mM. However, all strains produced roughly the same amounts of isopiperitenol and only traces of (-)-limonene were left after conversion. This indicated, that (-)-limonene was converted too quickly to show any difference between the strains. Therefore, we tested different (-)-limonene concentrations to optimise assay conditions and to see the maximal conversion rates of resting cells. For the preparation of the 100 mM (-)-limonene stock solution, DMSO was used as solvent with 1% Triton™ X-100. Both chemicals are toxic for *S. cerevisiae*. Hence, the concentration of the substrate was elevated in the stock solutions to keep DMSO concentration at 2 % and Triton™ X-100 concentrations at 0.02%. To compare the performance of different initial (-)-limonene concentrations in a conversion assay, initial (-)-limonene concentrations of 3, 5, 8, 10 and 15 mM were chosen.

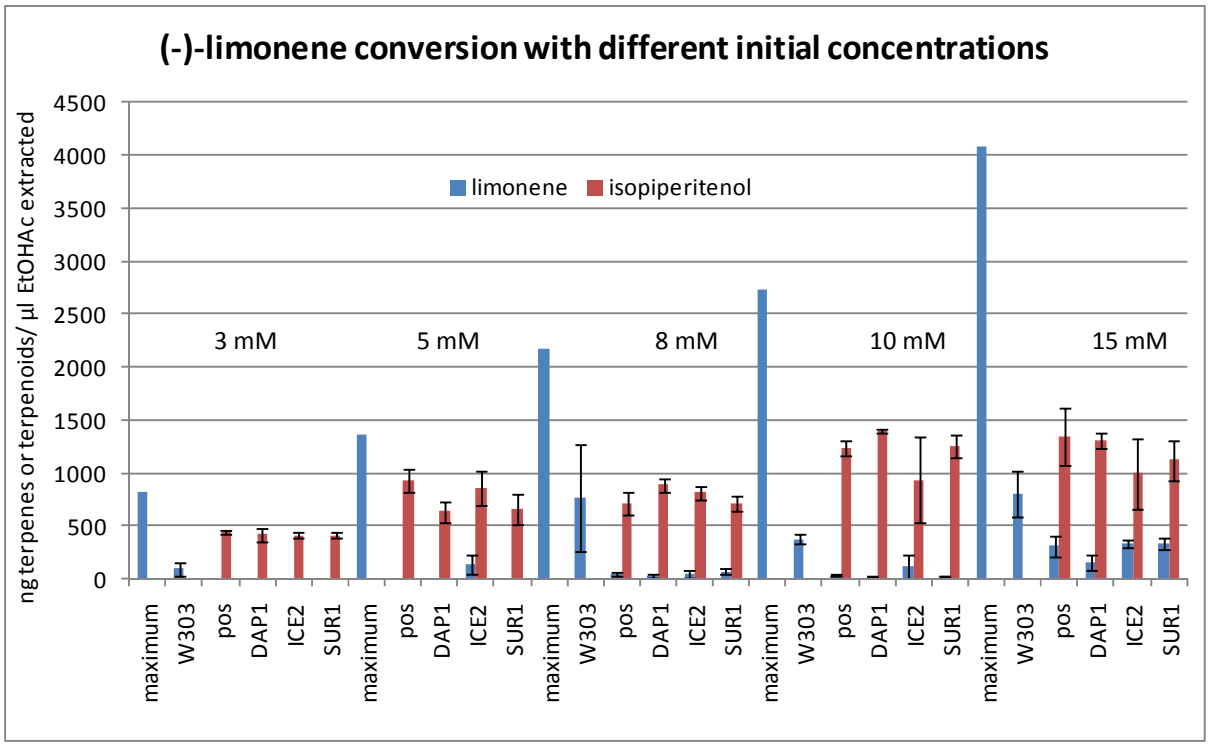

Figure 24: (-)-Limonene conversion assay with different initial (-)-limonene concentrations, max represents the initial (+)-valencene concentration, strains listed in Table 13 were tested, 2 biological and 4 technical replicates were tested per sample, data represented as means and standard deviation

None of the tested strains showed improved conversion compared to the positive control (Figure 25). However, the conversion assay showed that the strains tolerate (-)-limonene concentrations up to 15 mM. Up to a (-)-limonene concentration of 5 mM, approximately 2/3 of the substrate were converted. Higher substrate concentrations did not increase product formation. This effect could be due to product inhibition or a limited substrate transport into the cells. For further assays, (-)-limonene concentrations of 6 mM were chosen.

Conversion after 24 h induction

Anita Emmerstorfer had found out that overexpressing *ICE*2 had a stabilising effect on CPR over time [14]. The overexpression of *ICE*2 had no immediate effect on the activity of the PM17/CPR system in contrast to the HPO/CPR system (chapter 4.3 and 4.5.3) [14]. Hence, it was speculated that the beneficial effect of *ICE*2 for the PM17/CPR system could occur after a longer induction time. To check whether the co-expressed PM17/CPR were stable over a longer period of time due to *ICE*2 overexpression a conversion assay was performed with elongated induction time. Usually, the cells were induced with galactose for 6 h (chapter 0).

However, for this assay cells were induced for 24 h (Figure 26). W303 *MATα* P_{GAL1}-*ICE*2His_6 pESC URA P_{GAL1}-CPR-*myc* P_{GAL1}-PM17 opt.-Flag (*ICE*2H) was tested by Anita Emmerstorfer to perform as well as the untagged *ICE*2 strain [30].

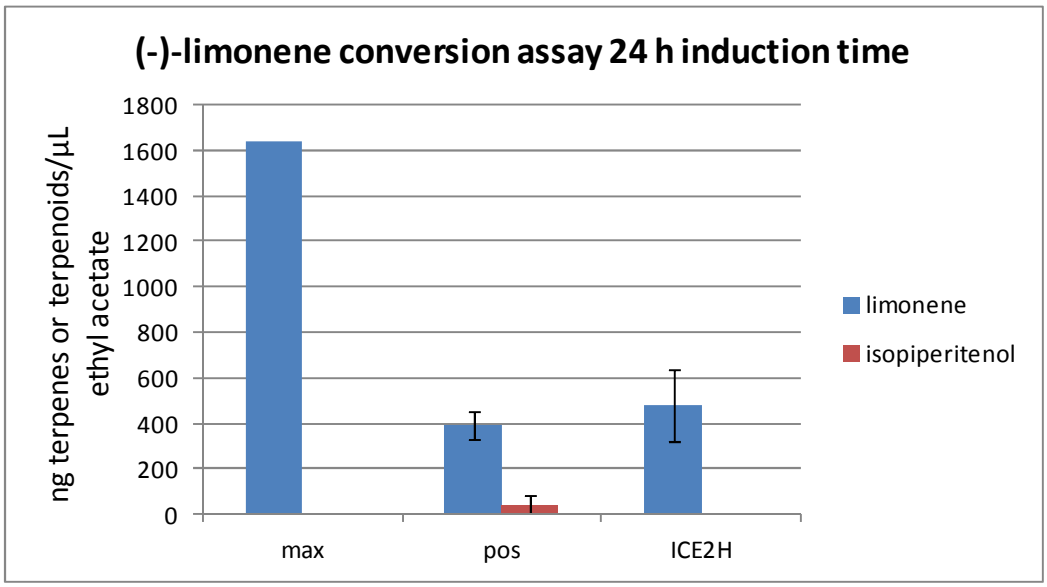

Figure 25: (-)-Limonene conversion after extending induction time to 24 h, max represents the initial (-)-limonene concentration, strains *ICE2* and the positive control (Table 13), 2 biological and 4 technical replicates were tested per sample, data represented as means and standard deviation

After 24 h of induction, no detectable amounts of isopiperitenol in *ICE*2H and hardly any in the positive control were found (Figure 26). Usually, after 6 h of induction, the positive control produced about 800 ng/µL isopiperitenol (Figure 25). These results indicate that the PM17/CPR system was not stable over 24 h. The overexpression of *ICE2* had no positive effect on the stability of the PM17/CPR system.

Conversion with different pH values

Previous studies within our group had revealed (+)-valencene hydroxylation by HPO/CPR was significantly improved by simply cultivating *P. pastoris* cells at pH 8 [21]. Therefore, influences of different pH values were also tested for the *S. cerevisiae* conversion system. During a normal conversion assay, the pH value of the buffer is roughly 7.4 (chapter 0). For this assay, the pH values of 50 mM KP_i, pH 7.4, were adjusted with NaOH or H_3PO_4 to pH 6, 8 and 9.

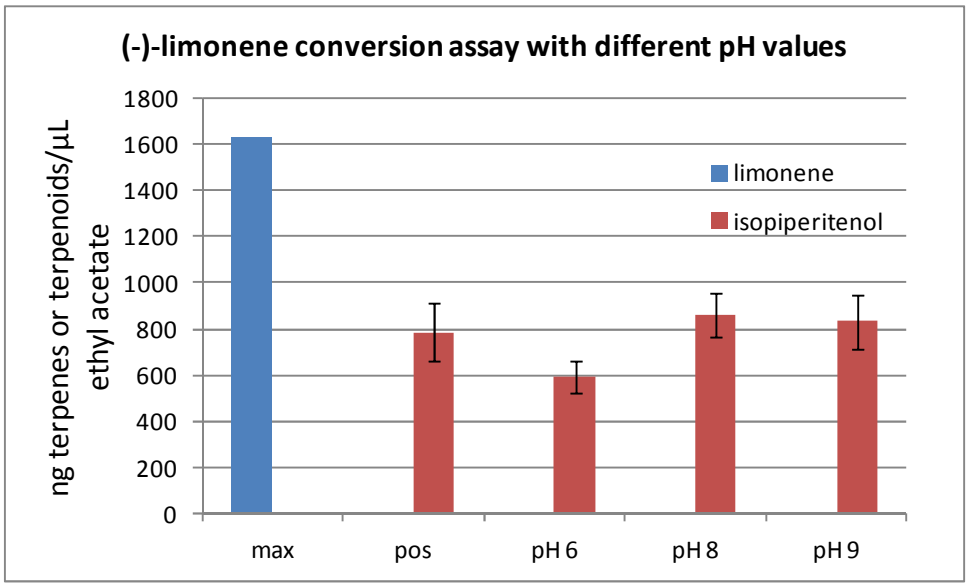

Figure 26: (-)-Limonene conversion with different pH values, max represents the initial (-)-limonene concentration, only the positive control (Table 13), pos was tested at pH 7.4, 2 biological and 4 technical replicates were tested per sample , data represented as means and standard deviation

Changing the pH value during (-)-limonene conversion in *S. cerevisiae* had only minor effects (Figure 27). A lower pH such as 6 showed decreased isopiperitenol production, whereas pH 8 showed insignificantly increased concentrations.

Conversions upon induction alternative carbon sources

Using glycerol as an alternative carbon source during the growth phase of the (+)-valencene conversion assay showed improved results (chapter 4.3). Therefore, seven different alternative carbon sources were tested in a (-)-limonene conversion assay. Acetate, citrate, ethanol, fructose, glycerol, lactate and sorbitol were chosen. Normally, cells were incubated in SD-URA medium containing 2% glucose for 48 h (chapter 0). During this assay cells were incubated in SD-URA medium containing 1% glucose for 24 h. Afterwards, 2% of alternative carbon sources were added and incubated for another 24 h and induced with galactose for 6 h. As a positive control, W303 *MATα* pESC URA P_{GAL1}-CPR-*myc* P_{GAL1}-PM17 opt.-Flag was chosen.

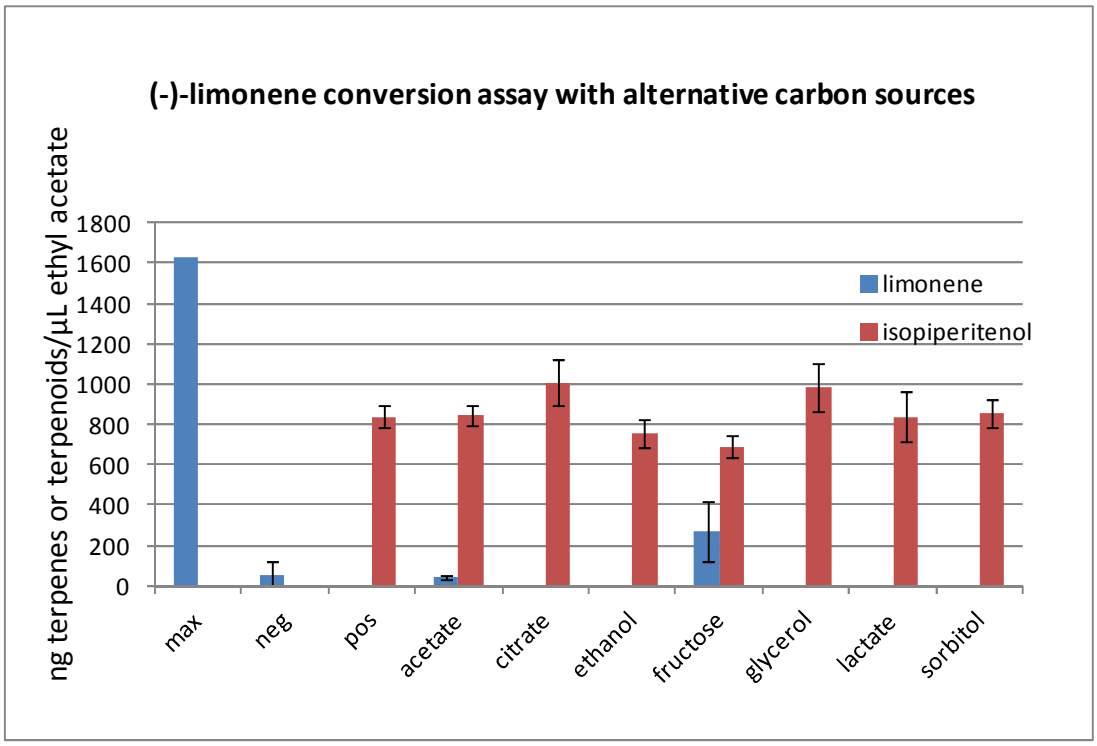

Figure 27: (-)-Limonene conversion with alternative carbon sources, max represents the initial (-)-limonene concentration, only the negative and positive control was tested (Table 13), pos is positive control under normal conditions, 2 biological and 4 technical replicates were tested per sample , data represented as means and standard deviation

As indicated in Figure 28, the addition of citrate and glycerol showed highly improved (-)-limonene conversion. Acetate, lactate and sorbitol led to roughly the same isopiperitenol concentrations as the positive control. Adding ethanol and fructose resulted in decreased isopiperitenol production. A Western Blot analysis was performed with cells after the conversion (Figure 29) analysis revealed no changes in the expression levels of PM17. Also, the differences in the CPR band intensities was supposedly due to slightly different amounts of loaded protein as suggested by the Ponceau S staining image. The varying outcomes of using different carbon sources in (-)-limonene conversion assays could not be correlated to changed expression levels of PM17/CPR.

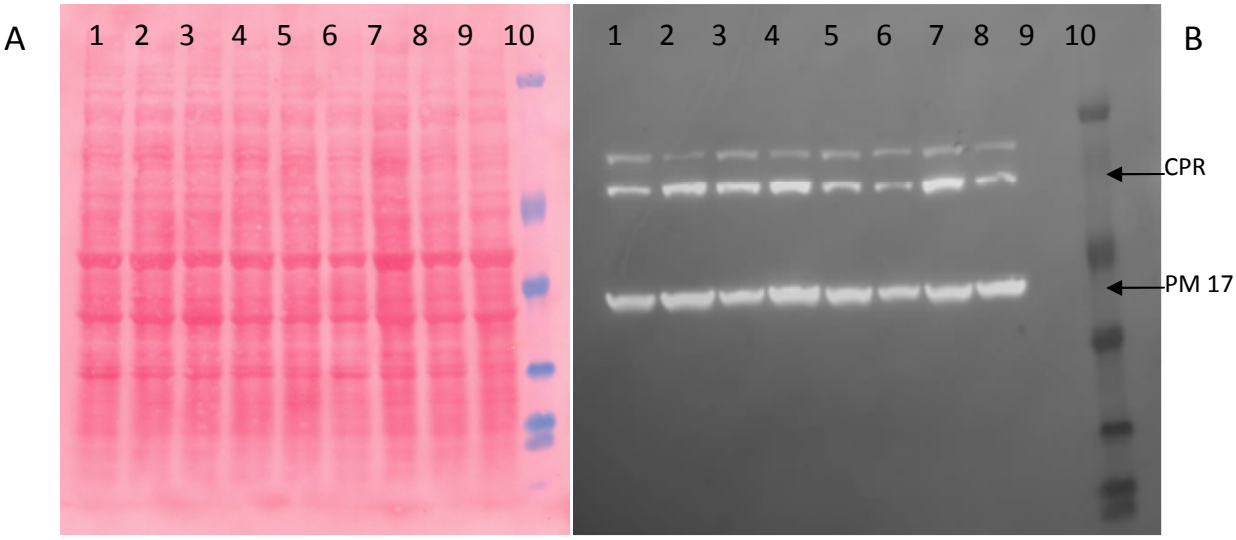

Figure 28: Western Blot analysis after conversion with cells grown with different carbon sources, A is Ponceau S staining image, B is chemilumescence image

Table 15: Samples tested via Western blot analysis (Figure 29)

1	W303 *MATα* pESC URA3 P_{GAL1}-CPR-*myc* P_{GAL1}-PM17 opt.-Flag sorbitol
2	W303 *MATα* pESC URA3 P_{GAL1}-CPR-*myc* P_{GAL1}-PM17 opt.-Flag lactate
3	W303 *MATα* pESC URA3 P_{GAL1}-CPR-*myc* P_{GAL1}-PM17 opt.-Flag glycerol
4	W303 *MATα* pESC URA3 P_{GAL1}-CPR-*myc* P_{GAL1}-PM17 opt.-Flag fructose
5	W303 *MATα* pESC URA3 P_{GAL1}-CPR-*myc* P_{GAL1}-PM17 opt.-Flag ethanol
6	W303 *MATα* pESC URA3 P_{GAL1}-CPR-*myc* P_{GAL1}-PM17 opt.-Flag citrate
7	W303 *MATα* pESC URA3 P_{GAL1}-CPR-*myc* P_{GAL1}-PM17 opt.-Flag acetate
8	W303 *MATα* pESC URA3 P_{GAL1}-CPR-*myc* P_{GAL1}-PM17 opt.-Flag
9	W303 *MATα*
10	Page Ruler™ Prestained Ladder, ThermoScientific

Conversion with different over-expressed genes

New strains were constructed with the target genes *KAR2*, *LHS1*, *MXR1* and *RAD52* controlled by the *GAL1*-promoter and containing the PM17/CPR co-expression plasmid. Firstly, P_{GAL1} was inserted upstream of the target gene into genome in W303 *Matα* cells. Next, positively transformed cells were transformed with vector pESC URA P_{GAL1}-CPR-*myc* P_{GAL1}-PM17 opt.-Flag. Expression of *RAD52* from P_{GAL1} had shown very good results for HPO-, PM17- and CYP2D6/CPR in *P. pastoris* [21]. *MXR1* performed well in (+)-valencene conversion assays and *LHS1* produced high amounts of trans-nootkatol in an (+)-valencene *in vivo* synthesis and conversion assay in *S. cerevisiae* [own unpublished results]. The tested strains are listed in Table 14.

Table 16: Strains tested in (-)-limonene conversion assay

ID	strain
pos	W303 *MATα* pESC URA pESC URA P_{GAL1}-CPR-*myc* P_{GAL1}-PM17 opt.-Flag
*KAR*2H	W303 *MATα* P_{GAL1}-*KAR*2His_6 pESC URA P_{GAL1}-CPR-*myc* P_{GAL1}-PM17 opt.-Flag
*LHS*1H	W303 *MATα* P_{GAL1}-*LHS1*His_6 pESC URA P_{GAL1}-CPR-*myc* P_{GAL1}-PM17 opt.-Flag
*MXR*1H	W303 *MATα* P_{GAL1}-*MXR*1His_6 pESC URA P_{GAL1}-CPR-*myc* P_{GAL1}-PM17 opt.-Flag
*RAD*52H	W303 *MATα* P_{GAL1}-*RAD*52His_6 pESC URA P_{GAL1}-CPR-*myc* P_{GAL1}-PM17 opt.-Flag

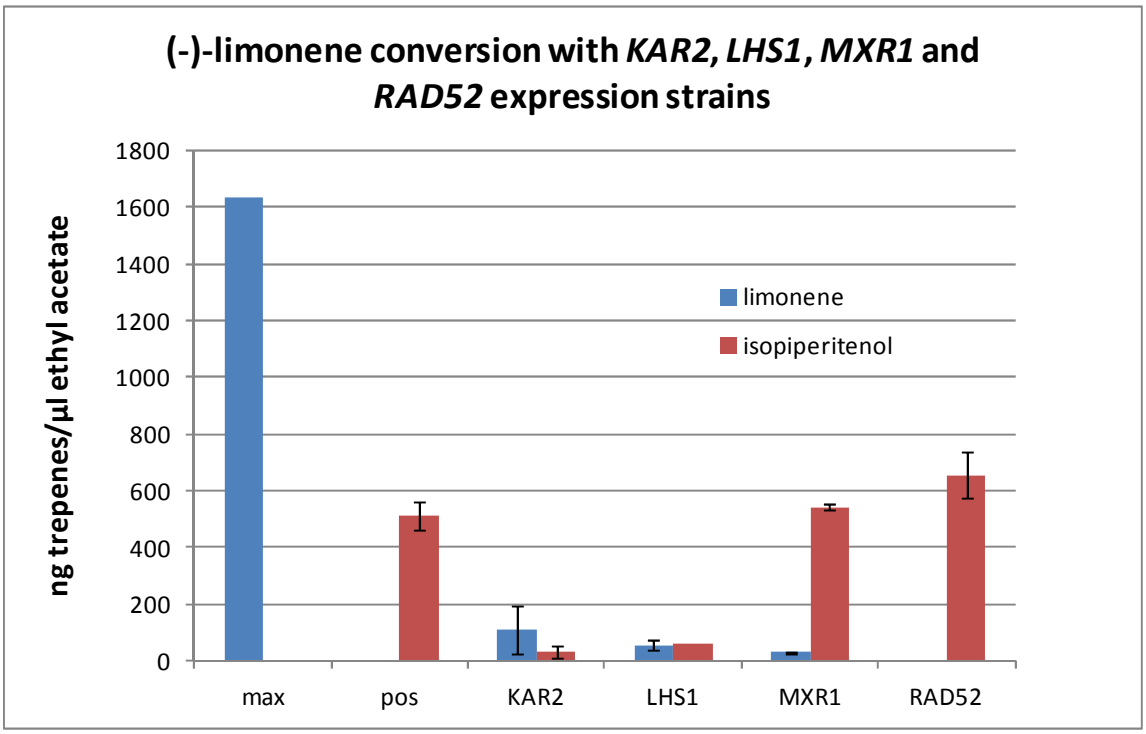

Figure 29: (-)-Limonene conversion assay with *KAR2*, *LHS1*, *MXR1* and *RAD52* expressed from P_{GAL1} (Table 16), 6 mM (-)-limonene was added as initial concentration, max represents the initial (-)-limonene concentration, 2 biological and 4 technical replicates were tested per sample, data represented as means and standard deviation

As depicted in Figure 30, strains expressing *KAR2* and *LHS1* from P_{GAL1} displayed low isopiperitenol concentrations. Both strains did not grow as well as the other strains. Usually, after 6 h of induction the cell cultures reached an OD_{600} of about 12. *KAR2* and *LHS1* strains only reached an OD_{600} of 8. The strain expressing *MXR*1 from P_{GAL1} produced roughly the same amount of isopiperitenol as the positive control. Strain *RAD52*, on the other hand,

showed slightly increased (-)-limonene conversion. It proved to be the best performing strain for (-)-limonene conversion for *S. cerevisiae* in this project.

4.5 BUFURALOL CONVERSION

CYP2D6 activity in bufuralol conversion was measured with whole cells in a resting cells assay. Conversion took place at 30°C for 30 min and was stopped by spinning the cells at full speed at 4°C for 10 min in a table top centrifuge. After addition of the internal standard, the supernatant was measured directly via HPLC-MS as bufuralol, 1-hydroxybufuralol and internal standard are water-soluble.

This assay was performed as described by Martina Geier, who had tested it in different hosts [8]. *S. cerevisiae* W303 *MATa* pESC P_{GAL1}-2D6 P_{GAL1}-CPR displayed an activity of 0.74 mU per g CDW.

Quantification of 1-hydroxybufuralol

To determine the concentrations of 1-hydroxybufuralol and bufuralol after the conversion, samples were measured with HPLC-MS. In a HPLC chromatogram, the peak areas are proportional to the concentration of the substance. The concentrations of substrate and product were calculated by comparing the respective peak areas with the internal standard prednisolone. The internal standard was added to a final concentration of 50 ng/µL. An example of chromatograms generated by a bufuralol conversion assay is shown in Figure 31.

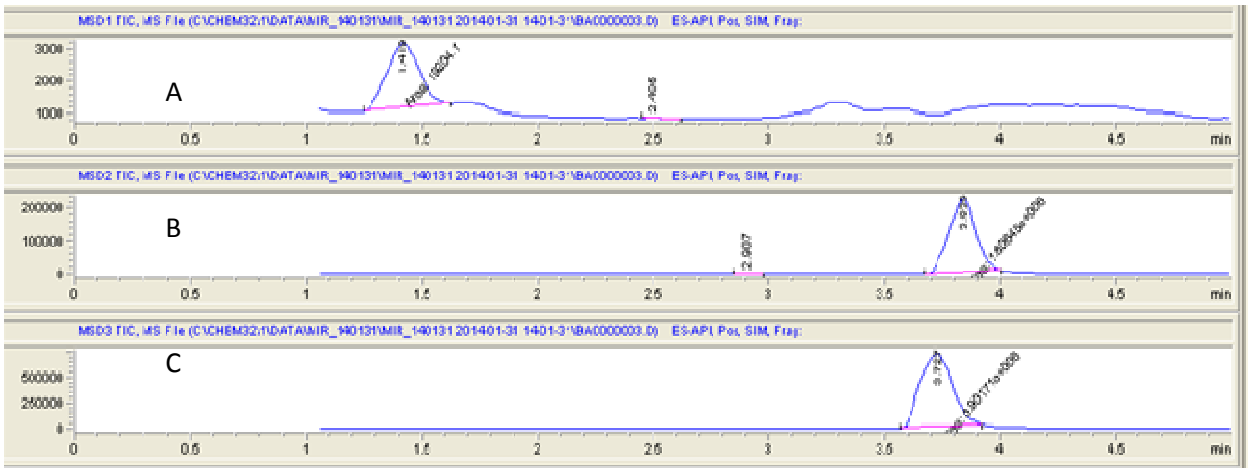

Figure 30: HPLC chromatogram of a sample of a bufuralol conversion assay (FIgure 33) , (A) 1-hydroxybufuralol, (B) bufuralol and (C) prednisolone, Retention times are: 1.4 min for 1-hydroxybufuralol, 3.8 min for bufuralol and 3.7 min for prednisolone

Improvement of bufuralol conversion assay

At first, the bufuralol conversion assay was performed exactly according to Geier et al. (2012) [8]. However, very low CYP2D6 activity was calculated. To improve assay performance, a new plasmid with optimized genes (optimized for *P. pastoris* by Tamara Wriessnegger) was cloned. The outcome of conversion assays with the optimized plasmid were still not as high as described in Geier et al (2012). Therefore, the amount of cells used in the assay was reduced from 75 to 20 OD_{600} units.

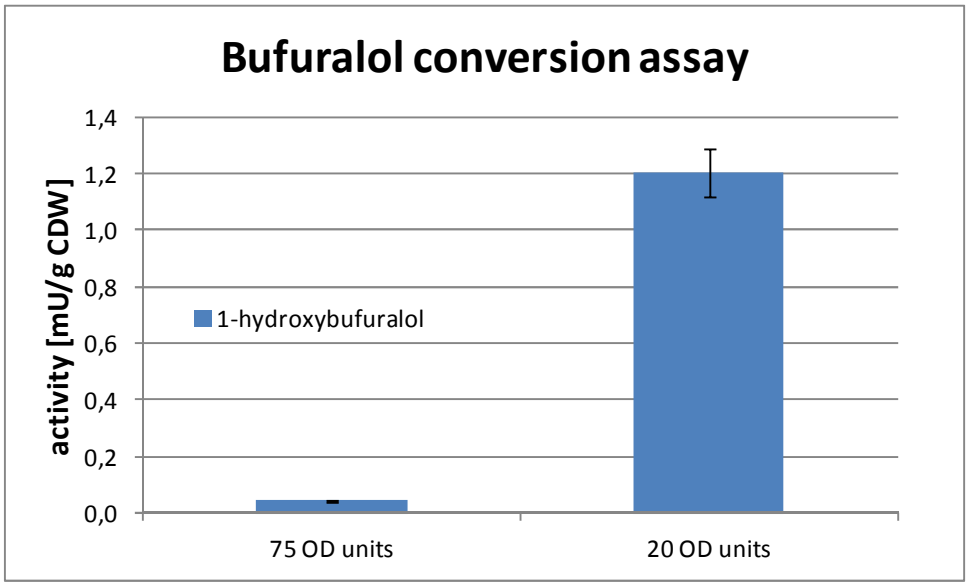

Figure 31 : CYP2D6 activity with 75 and 20 OD600 units of cells, 2 biological and 3 technical replicates were tested per sample , data represented as means and standard deviation

Reducing the amount of cells to nearly a quarter of the original amount resulted in a 25-fold improvement of specific activity (Figure 32). The subsequent bufuralol conversion assays were carried out with 20 OD_{600} units.

To determine the CYP2D6 activity under optimal conditions, high concentrations of bufuralol were added for the conversion. Less than 1% of total bufuralol was converted to 1-hydroxybufuralol. Hence, we wanted to know, if 1-hydroxybufuralol had been held back in the cells. After conversion, the cells were lysed with glass beads, pelleted and the supernatant was prepared for HPLC-MS measurement.

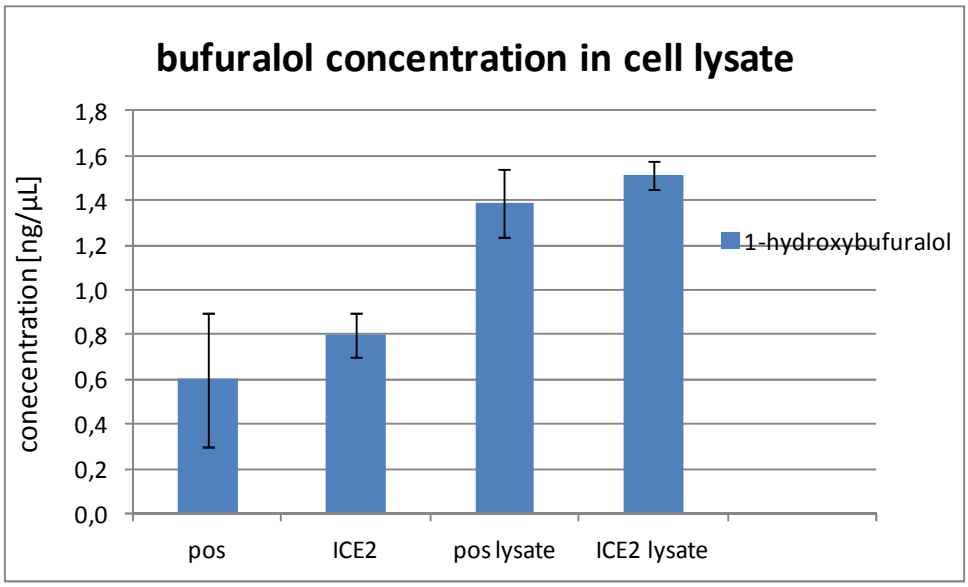

Figure 32: HPLC-MS measurement from the same samples directly after conversion and after an additional cell lysis, 2 biological and 3 technical replicates were tested per sample, data represented as means and standard deviation

After cell lysis with glass beads, the cumulative 1-hydroxybufuralol concentrations found in the supernatants were roughly two times higher than before cell lysis (Figure 33). However, the concentrations of 1-hydroxybufuralol after cell lysis were always considerably higher. Therefore, the conclusion was drawn that the product was indeed held back in the cells.

Performance of different over-expression strains

For the following bufuralol conversion assays, the newly cloned pESC URA P_{GAL1}-hCPR–*myc* P_{GAL1}-CYP2D6-Flag with optimized hCPR and CYP2D6 genes was used. Based on good results in (+)-valencene conversion assays performed by Anita Emmerstorfer [30], a strain expressing *ICE2* from P_{GAL1} was tested in a bufuralol conversion assay. A *RAD*52 strain showed good results for bufuralol conversion in *P. pastoris* [21] [21]. Kar2p and Lhs1p had not been tested for these systems yet.

Table 17: Strains tested in bufuralol conversion assays

ID	Strain
pos	W303 *MATα* pESC URA P_{GAL1}-hCPR –*myc* P_{GAL1}-CYP2D6-Flag
ICE2	W303 *MATα* P_{GAL1}-*ICE2*His_6 pESC URA P_{GAL1}-hCPR –*myc* P_{GAL1}-CYP2D6-Flag
KAR2	W303 *MATα* P_{GAL1}-*KAR2*His_6 pESC URA P_{GAL1}-hCPR –*myc* P_{GAL1}-CYP2D6-Flag
LHS1	W303 *MATα* P_{GAL1}-*LHS1H*is_6 pESC URA P_{GAL1}-hCPR –*myc* P_{GAL1}-CYP2D6-Flag
RAD52	W303 *MATα* P_{GAL1}-*RAD52*His_6 pESC URA P_{GAL1}-hCPR –*myc* P_{GAL1}-CYP2D6-Flag

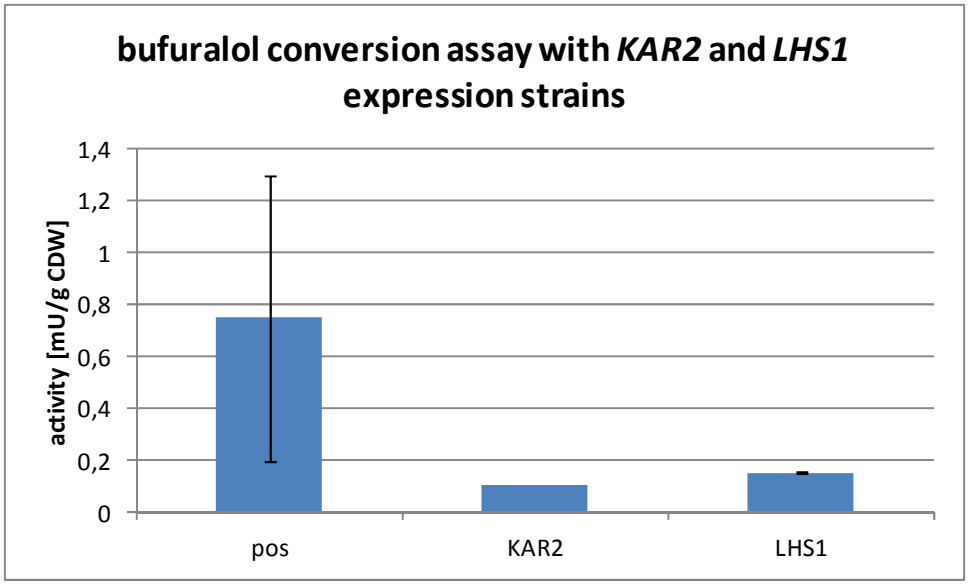

Figure 33: Bufuralol conversion assay with *KAR2* and *LHS1* strains and positive control (Table 17), 2 biological and 3 technical replicates were tested per sample , data represented as means and standard deviation

In comparison with the positive control both *KAR*2H and *LHS1H* displayed very low CYP2D6 activity (Figure 34). Like in the (-)-limonene conversion assay, both strains reached only an optical density of around 8. On the other hand, strains expressing ICE2 and RAD52 from P_{GAL1} performed much better in an independent assay (Figure 35). In the former assay the positive control showed an activity of 0.75 mU/g CDW compared to 1.75 mU/g CDW in this one. The *ICE2* strain exhibited an improved activity of 2.19 mU/g CDW, whereas the *RAD52* strain stayed with 1.56 mU/g CDW below the activity of the positive control. A Western Blot analysis was performed with strains expressing *ICE2* and RAD52 from P_{GAL1} after conversion.

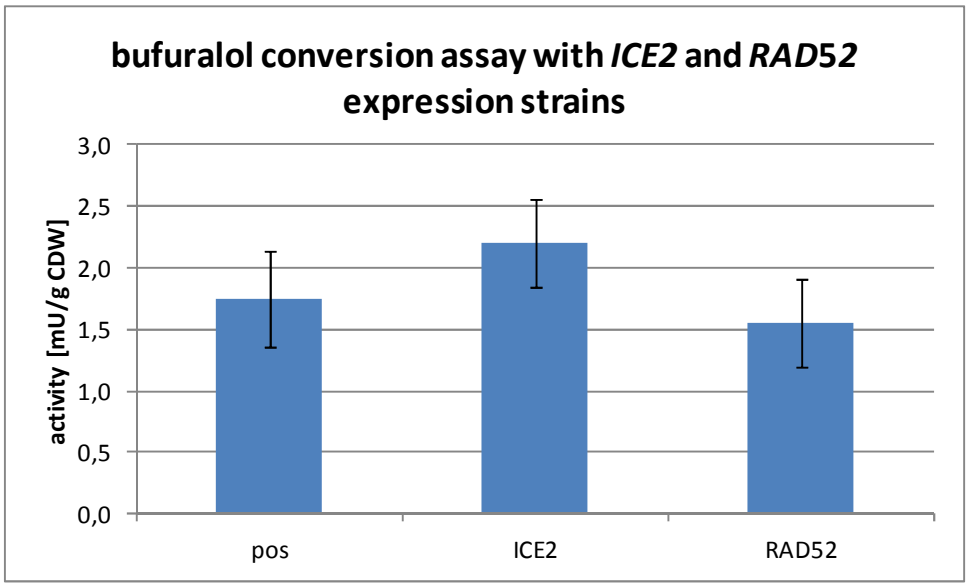

Figure 34: Bufuralol conversion assay with strains expressing *ICE2* and *RAD52* from P_{GAL1} and postive control (Table 17), 2 biological and 3 technical replicates were tested per sample, data represented as means and standard deviation

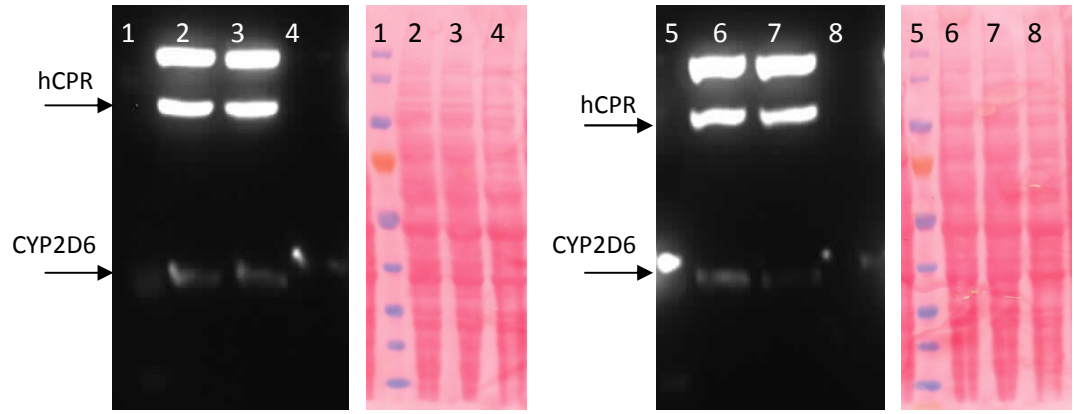

Figure 35: Western Blot analysis of strains expressing *ICE2* and *RAD52* from P_{GAL1} and negative and positive control

Table 18: Samples tested via Western blot analysis (Figure 36)

1	Page Ruler™ Prestained Ladder, ThermoScientific
2	W303 *MATα* pESC URA P_{GAL1}-hCPR –*myc* P_{GAL1}-CYP2D6-Flag
3	W303 *MATα* P_{GAL1}-*ICE2*His_6 pESC URA P_{GAL1}-hCPR-*myc* P_{GAL1}-CYP2D6-Flag
4	W303 *MATα*
5	Page Ruler™ Prestained Ladder, ThermoScientific
6	W303 *MATα* pESC URA P_{GAL1}-hCPR –*myc* P_{GAL1}-CYP2D6-Flag
7	W303 *MATα* P_{GAL1}-*RAD52*His_6 pESC URA P_{GAL1}-hCPR –*myc* P_{GAL1}-CYP2D6-Flag
8	W303 *MATα*

The band intensities of CPR were much higher than for CYP2D6. There were no differences between the expression levels of CYP2D6 or hCYP in *ICE2*, *RAD52* or the positive control. The differences in the CYP2D6/hCPR activity could not be explained by differences on the protein level.

4.6 CO-DIFFERENCE SPECTRA

Microsomal fractions were isolated to monitor CYP450 expression by recording CO-difference spectra. CYP450s have a distinct band at 450 nm when carbon-monoxide is bound, which enables quantification of the enzymes. Firstly, when measuring the CO-difference spectrum, a baseline is taken before the microsome preparations are exposed to carbon-monoxide (chapter 3.13). Afterwards, the preparations are fumigated with CO and the actual spectrum is measured. In **Figure 36** the following strains were tested: positive control and a strain expressing ICE2 from P_{GAL1} for the PM17/CPR system and the positive control for the CYP2D6/hCPR system.

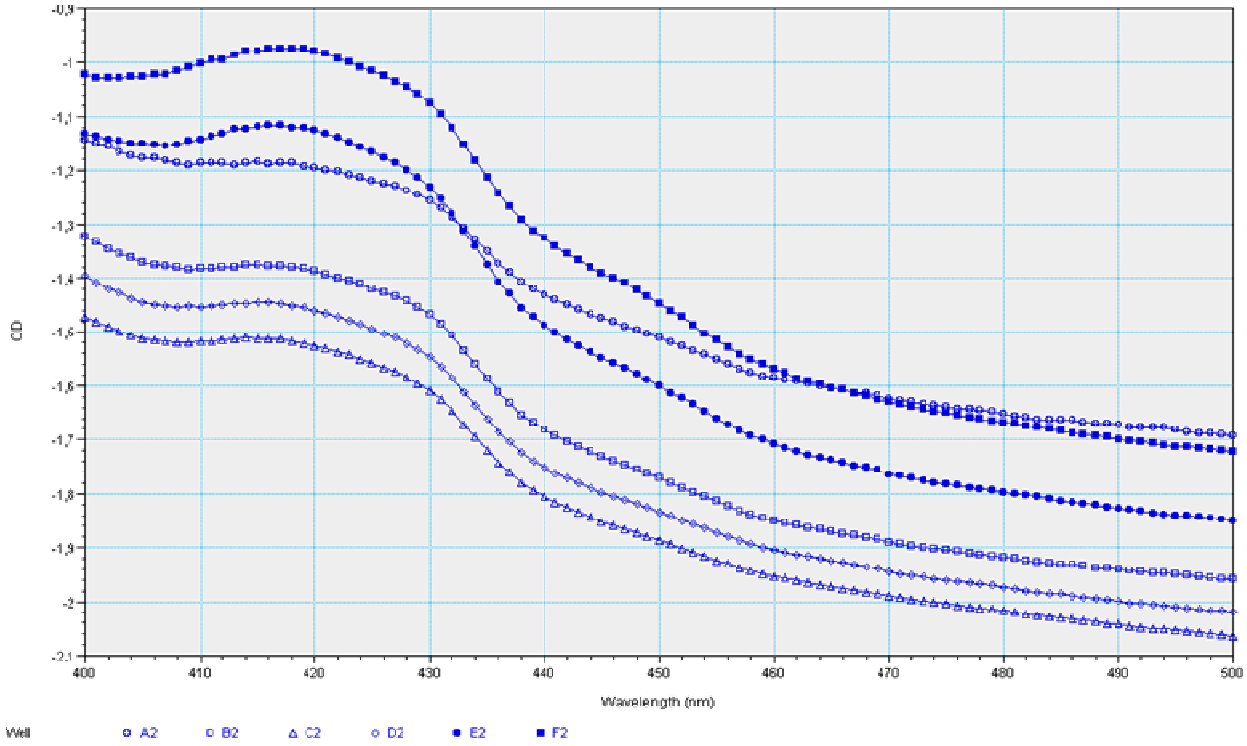

Figure 36: CO-difference spectrum; pos PM17: A2 and B2, *ICE2* PM17: C2 and D2, pos CYP2D6: E2 and F2;

As indicated in Figure 37, no distinctive peaks were found at 450 nm. Thus, amounts of P450 enzymes produced in *S. cerevisiae* are too low to be quantified by available equipment.

5. DISCUSSION

5.1 (+)-VALENCENE CONVERSION

To improve the (+)-valencene conversion assay with resting cells, two general approaches were chosen. Changing the conditions during cultivation by adding ethanol and glycerol as alternative carbon sources and over-expression of *ICE*2. Whereas the addition of ethanol led to decreased conversion, adding glycerol and over-expressing *ICE*2 led to improved results.

S. cerevisiae cells are able to survive ethanol concentrations of up to 16%. Ethanol targets the plasma membrane which causes higher fluidity and at higher concentrations ultimately leads to an influx of protons [31]. This disrupts the electrochemical gradient across the plasma membrane resulting in decreased growth rates and cell viability. Additionally, ethanol causes oxidative stress by generating reactive oxygen species such as superoxide, hydroxyl radicals and hydrogen peroxide [32]. During this project, ethanol concentrations of 2% were tested. Adding ethanol resulted in slightly higher growth rates and lower HPO activity. Although not lethal, ethanol still affected HPO activity negatively (Figure 19). One reason could be the destabilizing effect of ethanol on plasma membranes. However, other membranes within the cell could be affected by ethanol too. As HPO is attached to the ER membrane, this could cause lower conversion rates. However, the impact of the oxidative stress might be much more severe. HPO´s reactive site contains an iron-sulfur-complex which is very sensitive to oxidative stress.

Adding glycerol to preparations of beef liver NADPH-cytochrome P450 reductase preparations had a stabilizing effect on this enzyme [33]. Arinc et al. (2002) tested the CPR activity over time at two different temperatures and confirmed the stabilizing effect for both, 25 and 37°C. The improved stability of CPR could be beneficial for the conversion of (+)-valencene by HPO (Figure 19). Overexpressing *ICE2* seems to target CPR activity and stability. Ice2p is an integral membrane protein involved in maintenance and distribution of the cortical ER network [20]. Anita Emmerstorfer found out that the activity of CPR remained higher over time in *ICE*2 over-expression strains [30]. The mechanism of this effect remains to be elucidated.

5.2 (-)-LIMONENE *IN VIVO* SYNTHESIS

At a previous stage of this project, (-)-limonene *in vivo* synthesis employing (-)-limonene synthase had already been tried [14]. However, no (-)-limonene could be detected via GC-FID measurement. Therefore, a codon optimization for expression in *P. pastoris* was performed by Tamara Wriessnegger and new strains were constructed. To provide a sufficient amount of geranyldiphosphate for (-)-limonene synthesis t*HMG*1 was over-expressed. Unfortunately, no (-)-limonene was detected. (-)-Limonene is a highly volatile substance and it was speculated that the *in vivo* synthesised product might vaporize before detection. To prevent vaporization, strains which simultaneously expressed LimS and the PM17/CPR system were constructed, as isopiperitenol should be less volatile then (-)-limonene. The idea was that (-)-limonene could directly be converted to isopiperitenol which could be measured instead. Nevertheless, no isopiperitenol could be detected. Western blot analysis confirmed the expression of LimS. FPPS synthesises the farnesyl diphosphate out of two molecules isopentenyl diphosphate and one molecule dimethylallyl diphosphate [27]. Geranyl diphosphate is an intermediate of this reaction. It is suggested that geranyl diphosphate never leaves the catalytic site of FPPS and, therefore, is not available for LimS to form (-)-limonene. In order to make geranyl diphosphate available, separate geranyl diphosphate synthase and farnesyl diphosphate synthase have to be expressed in *S. cerevisiae*.

5.3 (-)-LIMONENE CONVERSION

(-)-Limonene conversion by resting cells was tested under different conditions such as varying (-)-limonene concentrations, pH values, elongated induction time and the addition of alternative carbon sources. The overexpression of *DAP1*, *ICE2*, *SUR1*, *KAR2*, *LHS1*, *MXR1* and *RAD52* was part of the metabolic engineering approach to generate higher conversion levels. A (-)-limonene concentration of 0.2 µg/mL was observed to result in half maximal growth of *S. cerevisiae* [34]. During this work, (-)-limonene conversion assays were only performed with resting cells in which the PM17/CPR system was found to work at concentrations up to 2.4 µg/mL. However, the amount of isopiperitenol in comparison to

the initial (-)-limonene concentration started to stagnate. Adding 0.7 µg/mL of (-)-limonene resulted in conversion rates of about 70%, whereas 1.1 µg/mL (-)-limonene was converted only to 50%. It seems that elevated (-)-limonene concentrations inhibit the production of isopiperitenol. (-)-limonene is described to target the cell wall causing a toxic effect [35]. How this toxic effect works and how it affects isopiperitenol production remains to be determined.

Changing the pH value during the growth phase from pH 6 to 8 had a beneficial effect on the CYP450 activity in *P. pastoris* [21] [21]. Therefore, the pH values were adjusted to pH 6, 7.4, 8 and 9 during the conversion with buffered *S. cerevisiae* resting cells. pH 8 and 9 resulted in slightly elevated isopiperitenol levels whereas pH 6 resulted in lower conversion rates. According to the website (http://www.brenda-enzymes.org/php/result_flat.php4?ecno=1.14.13.47) the pH optimum for limonene-3-hydroxylase is 7.4. In our studies, the activity of PM17 was only tested in resting cells assays and, therefore, the enzyme was protected by the cell from harsh environmental conditions such as changes of the pH value. Changing the pH values at this rate would have probably not directly affected the PM17/CPR system. Sandra Moser found out that a higher pH value lowered the cell wall stability of *P. pastoris* [21] [21]. This led to the assumption that a less stable cell wall led to enhanced transport of hydrophobic substances, like (-)-limonene and isopiperitenol. The effect was observed in *S. cerevisiae* at a much lower impact level. *S. cerevisiae* and *P. pastoris* have different cell wall compositions and to this date very little is known about *P. pastoris*` cell wall. The varying impact of pH values may be due to differences in cell wall composition between these two yeasts.

Anita Emmerstorfer investigated the stability of P450 enzymes and CPRs and could show that the activity of HPO correlated with the activity of CPR over time [30]. During this thesis, the induction time usually was set to be 6 h for the PM17/CPR system. After 24 h of induction no isopiperitenol formation was seen any more. This led to the conclusion that not enough functional PM17/CPR was left after 24 h.

Using glycerol as alternative carbon source resulted in improved performance of the HPO/CPR system as described earlier. Hence, other carbon sources were tested as well for the PM17/CPR system. Acetate, citrate, ethanol, fructose, glycerol, lactate and sorbitol were

chosen. Adding ethanol and fructose led to lower conversion rates. Acetate, lactate and sorbitol resulted in the same isopiperitenol formation rates as using only glucose as carbon source. On the other hand, addition of citrate and glycerol led to a better performance. The positive impact of glycerol and citrate on P450 hydroxylases had also been observed in *Pseudomonas putida* [36]. The nature of the positive influence of citrate and glycerol on the P450 enzyme activity remains to be elucidated.

Overexpressing *RAD*52 resulted in increased activity of all P450/CPR systems tested in this project in *P. pastoris* [21] [21]. Rad52p is involved in homologous recombination and DNA double-strand repair in *S. cerevisiae* [22]. However, these functions do not explain the improved PM17/CPR system activity. No elevated expression levels of PM17 or CPR could be shown via Western blot analysis compared to the positive control either. A protein-protein interaction study identified proteins which have not been associated with Rad52p before [37]. Four heat-shock proteins and three oxidation related proteins were identified. The CYP450´s heme-thiolate group is sensible to oxidative stress. Hence, the interaction of Rad52p with such proteins could result in better PM17 performance. The mechanism of how Rad52p influences P450 enzymes remains unclear.

DAP1, *ICE2* and *SUR1* expressed from P_{GAL1} were found to be beneficial for the conversion of (+)-valencene in *S. cerevisiae* [14]. However, for the PM17/CPR system no improvement was observed. This observation was confirmed at the protein level by Western blot analysis. The expression of PM17 or CPR was not improved by over-expressing any of the three genes (chapter 0). Ice2p is involved in maintenance of ER membranes. Sur1p plays a role in the sphingolipid biosynthesis which also affects membrane properties [19]. Dap1p is a heme-binding damage response protein and stably binds Erg11p and Erg5p which play important roles in the biosynthesis of ergosterol [38]. Hughes et al. (2007) found no other proteins binding Dap1 in yeast lysate. Overexpressing *DAP*1 in *S. cerevisiae* led to increased production of ergosterol which in turn might improve the ER membrane conditions for the HPO/CPR system. It seems that the PM17/CPR system is less influenced by changes in the ER membrane than the HPO/CPR system.

Mxr1p is a methionene-S-sulfoxide reductase which protects iron-sulfur clusters from oxidative inactivation [25]. It reduces the S-stereoisomer of methionine sulphoxide. In a

previous screening in *P. pastoris* the overexpression *MXR*1 led to an improvement of CYP450 activity (Tamara Wriessnegger, personal communication). Expressing *MXR1* from P_{GAL1} in *S. cerevisiae* did not result in improved CYP450 functions compared to the positive control. The catalytic site of PM17 contains a heme group with a cystein thiolate group as the fifth ligand of the heme iron [1]. Hence, it could be that Mxr1p is not able to reduce a cystein thiolate group and thus, has no effect on PM17. There is no published information on the effect of Mxr1p an P450 enzymes.

The strains expressing *KAR2* and *LHS1* from P_{GAL1} did not grow as well as the other strains and isopiperitenol concentrations were very low after the PM17/CPR - conversions. Kar2p and LHS1p are both chaperones of the HSP70 family found in the lumen of the ER. Their expression is triggered by the unfolded protein response (UPR) in which unfolded protein is blocking the ER [23], [24]. In the engineered strains, the endogenous target genes are under the control of the galactose promoter and repressed if grown on glucose. This may explain the decreased growth rate of the cells before induction and could be a reason for the low (-)-limonene conversion. Proteotoxicity caused by accumulation of unfolded protein could negatively affect the PM17/CPR system.

5.4 Bufuralol Conversion

The bufuralol conversion assay was improved by reducing the amount of cells and using codon optimized genes. Over-expression of *ICE2*, *KAR2*, *LHS1* and *RAD52* was tested and the concentration of 1-hydroxybufuralol was measured before and after cell lysis. Reducing the amount of cells used in the assay from 75 to 20 OD_{600} units resulted in a 25-fold improvement in specific CYP2D6 activity. Additionally, more 1-hydroxybufuralol was found after cell lysis in the supernatant than before. These findings led to the conclusion that bufuralol and 1-hydroxybufuralol are somehow retained in *S. cerevisiae* cells. Oxygen limitation could be another explanation for this effect (Martina Geier, personal communication).

The expression of *KAR2* and *LHS1* from P_{GAL1} resulted in very poor CYP2D6 activity. Again, the strains exhibited lower growth rates. Overexpression of *ICE2* resulted in elevated CYP2D6 activity, while overexpression of *RAD52* led to decreased activity. This outcome is inverse compared to the PM17/CPR system and leads to the conclusion that PM17 and

CYP2D6 are influenced by different environmental factors despite being members of the same protein superfamily.

5.5 SUMMARY

Table 19: Alternative carbon sources tested in resting cells assays and their effect (n. d. not determined)

Carbon source	(+)-Valencene conversion	(-)-Limonene conversion
acetate	n. d.	no effect
citrate	n. d.	positive effect
ethanol	negative effect	negative effect
fructose	n. d.	negative effect
lactate	n. d.	no effect
glycerol	positive effect	positive effect
sorbitol	n. d.	no effect

It seems that adding citrate, ethanol or glycerol may have a general effect on P450 enzymes (Table 19). It would be interesting to test citrate and glycerol on HPO-, PM17- and CYP2D6/CPR systems and observe if combining them could further increase the positive outcome. Another experiment that could be conducted would be the addition of glycerol or citrate to already improved overexpression strains to check for higher activity.

Table 19: Over-expressed genes tested in resting cells assays and their effect (n. d. not determined)

Gene	(+)-Valencene	(-)-Limonene	Bufuralol
*DAP*1	positive effect [14]	no effect	n. d.
ICE2	positive effect [14]	no effect	positive effect
KAR2	negative effect	negative effect	negative effect
LHS1	no effect	negative effect	negative effect
MXR1	negative effect	no effect	n. d.
RAD52	positive effect [14]	positive effect	no effect
SUR1	positive effect [14]	no effect	n. d.

During this project no gene was found which was able to improve the activity of all three CYP/CPR systems in *S. cerevisiae*. This leads to the conclusion that despite belonging to the same protein superfamily HPO, PM17 and CYP2D6 are affected differently by changes in their cellular environment. However, the overexpression of *ICE2* and *RAD52* led to the improvements in 4 and in 5 out of 6 tested systems in *S. cerevisiae* and *P. pastoris*, respectively [21], [30]. For industrial applications strains overexpressing *ICE*2 and *RAD*52 should be tested in batch systems in future experiments.

6. REFERENCES

[1] Rita Bernhardt, Frank Hannemann, Andreas Bichet, Kerstin M. Ewen, "Cytochrome P450 systems—biological variations of electron transport chains," *Biochimica et Biophysica Acta (BBA) - General Subjects,* vol. 1770, no. 3, pp. 330-344, March 2007.

[2] Sibylle Brenner, Sam Hay, Andrew W. Munro and Nigel S. Scrutton, "Inter-flavin electron transfer in cytochrome P450 reductase – effects of solvent and pH identify hidden complexity in mechanism," *FEBS Journal,* vol. 275, p. 4540–4557, July 2008.

[3] Bernard Meunier, Samue¨l P. de Visser, and Sason Shaik, "Mechanism of Oxidation Reactions Catalyzed by Cytochrome P450 Enzymes," *Chemical Reviews,* no. 104, pp. 3947-3980, August 2004.

[4] Shunji Takahashi, Yun-Soo Yeo, Yuxin Zhao, Paul E. O'Maille, Bryan T. Greenhagen, Joseph P. Noel, Robert M. Coates§, and Joe Chappell, "Functional Characterization of Premnaspirodiene Oxygenase, a Cytochrome P450 Catalyzing Regio- and Stereo-specific Hydroxylations of Diverse Sesquiterpene Substrates," *THE JOURNAL OF BIOLOGICAL CHEMISTRY,* vol. 282, no. 43, p. 31744–31754, October 2007.

[5] Yoshinori Asakawa, Mai Furusawa, Toshihiro Hashimoto, Yoshiaki Noma, "Highly Efficient Production of Nootkatone, the Grapefruit Aroma from Valencene, by Biotransformation," *Chemical and Pharmaceutical Bulletin,* vol. 53, no. 11, p. 1513—1514, November 2005.

[6] Matthias Wüst, Dawn B. Little, Michel Schalk, and Rodney Croteau, "Hydroxylation of Limonene Enantiomers and Analogs by Recombinant (2)-Limonene 3- and 6-Hydroxylases from Mint (Mentha) Species: Evidence for Catalysis within Sterically Constrained Active Sites," *Archives of Biochemistry and Biophysics,* vol. 387, no. 1, pp. 125-136, March 2001.

[7] R. Eccles, "Role of cold receptors and menthol in thirst, the drive to breathe and arousal," *Appetite,* vol. 34, no. 1, pp. 29-35, February 2000.

[8] Martina Geier, Andreas Braun, Anita Emmerstorfer, Harald Pichler, and Anton Glieder, "Production of human cytochrome P450 2D6 drug metabolites with recombinant microbes – a comparative study," *Biotechnology Journal,* vol. 7, no. 11, p. 1346–1358, November 2012.

[9] T. H. Pringle, R. J. Francis, P. B. East & R. G. Shanks, "Pharmacodynamic and pharmacokinetic studies on bufuralol in man," *British Journal of Clinical Pharmacology,* vol. 22, no. 5, pp. 527-534, 1986.

[10] Wouter A Duetz, Jan B van Beilen and Bernard Witholt, "Using proteins in their natural environment: potential and limitations of microbial whole-cell hydroxylations in applied biocatalysis," *Current Opinion in Biotechnology,* vol. 12, no. 4, p. 419–425, August 2001.

[11] Susan Zelasko, Amrita Palaria, Aditi Das, "Optimizations to achieve high-level expression of cytochrome P450 proteins using *Escherichia coli* expression systems," *Protein Expression and Purification,* vol. 92, no. 1, pp. 77-87,November 2013.

[12] A. Emmerstorfer, Membrane Protein Expression in E. coli, Master´s thesis TU Graz, Institut für Molekulare Biotechnologie, 2010.

[13] Patrick R. Arsenault, Kristin K. Wobbe, and Pamela J. Weathers, "Recent Advances in Artemisinin Production Through Heterologous Expression," NIH Public Access, Author Manuscript, 2010.

[14] A. Emmerstorfer, Improving heterologous cytochrome P450 functionality in *S. cerevisiae*, PhD thesis, TU Graz, Institut für Molekulare Biotechnologie, 2014.

[15] Glick, Bernard R.; Pasternak, Jack J.; Patten, Cheryl L., J. J. Pasternak and C. L. Patten, Molecular biotechnology, Washington, DC: ASM Press, 2010.

[16] Jacob Verghese, Jennifer Abrams, Yanyu Wang, Kevin A. Morano, "Biology of the Heat Shock Response and Protein Chaperones: Budding Yeast (*Saccharomyces cerevisiae*) as a Model System," *Microbiology and Molecular Biology Reviews,* vol. 76, no. 2, pp. 115-158, June 2012.

[17] Johann Wolfgang Goethe-University Frankfurt Institute for Molecular Biosciences, "EUROSCARF," SRD - Scientific Research and Development GmbH, 29 August 2013. [Online]. Available: www.euroscarf.de. [Accessed 13 Juni 2014].

[18] Rolf J. Craven, Julia C. Mallory, Gerard Crudden, Ben L. Johnson, Caiqing Mo, Charles A. Pierson, Martin Bard, "Dap1p, a Heme-Binding Protein That Regulates the Cytochrome P450 Protein Erg11p/Cyp51p in *Saccharomyces cerevisiae*," *Molecular and Cellular Biology,* vol. 25, no. 5, p. 1669–1679, March 2005.

[19] T. J. Beeler, D. Fu á J. Rivera, E. Monaghan, K. Gable, T. M. Dunn, "SUR1 (CSG1 / BCL21), a gene necessary for growth of *Saccharomyces cerevisiae* in the presence of high Ca2+ concentrations at 37° C, is required for mannosylation of inositolphosphorylceramide," *Mol Gen Genet,* vol. 255, no. 6, pp. 570-579, June 1997.

[20] Paula Estrada de Martin, Yunrui Du, Peter Novick and Susan Ferro-Novick, "Ice2p is important for the distribution and structure of the cortical ER network in *Saccharomyces cerevisiae*," *Journal of Cell Science,* vol. 118, pp. 65-77, January 2005.

[21] S. Moser, Engineering of the yeast *Pichia Pastoris* for improved terpenoid production, Master´s thesis, TU Graz, Institut für Molekulare Biotechnologie, 2014.

[22] Uffe H. Mortensen, Michael Lisby and Rodney Rothstein, "*Rad52*," *Current Biology,* vol. 19, no. 16, p. R676–R677, August 2009.

[23] Chia-Ling Hsua, Rupali Prasada, Christie Blackmanb, and Davis T. W. Nga, "Endoplasmic reticulum stress regulation of the Kar2p/BiP chaperone alleviates proteotoxicity via dual degradation pathways," *Molecular Biology of the Cell,* vol. 23, no. 4, pp. 630-641, February 2012.

[24] Nina Saris, Heidi Holkeri, Rachel A. Craven, Marja Makarow, "The Hsp70 Homologue Lhs1p Is Involved in a Novel Function of the Yeast Endoplasmic Reticulum, Refolding and Stabilization of Heat-denatured Protein Aggregates," vol. 137, no. 4, pp. 813-824, May 1997.

[25] Theodora C. Sideri, Sylvia A. Willetts and Simon V. Avery, "Methionine sulphoxide reductases protect ironsulphur clusters from oxidative inactivation in yeast," *Microbiology,* vol. 155, p. 612–623, February 2009.

[26] T. Polakowski, U. Stahl, C. Lang, "Overexpression of a cytosolic hydroxymethylglutaryl-CoA reductase leads to squalene accumulation in yeast," *Applied Microbiology and Biotechnology,* vol. 49, no. 1, pp. 66-71, January 1998.

[27] Marc J. C. Fischer, "Metabolic Engineering of Monoterpene Synthesis in Yeast," *Biotechnology and Bioengineering,* vol. 108, no. 8, p. 1883–1892, August 2011.

[28] Anton Horvath, Howard Riezmann, "Rapid Protein Extraction from *Saccharomyces cerevisiae*," *Yeast,* vol. 10, pp. 1305-1310, April 1994.

[29] R. Daniel Gietz, Robin A. Wood, "Transformation of yeast by lithium acetate/single-stranded carrier DNA/polyethylene glycol method," *Methods in Enzymology,* vol. 350, pp. 87-96, July 2002.

[30] Anita Emmerstorfer, Miriam Wimmer, Tamara Wriessnegger, Erich Leitner, Monika Müller, Iwona Kaluzna, Martin Schürmann, Daniel Mink, Guenther Zellnigd, Helmut Schwab, Harald Pichler, "Over-expression of *ICE2* improves biohydroxylation of (+)-valencene and stabilizes cytochrome P450 reductase levels in *Saccharomyces cerevisiae* and *Pichia pastoris*".*Publication in Progress.*

[31] Michael J. Anderson, Sarah L. Barker, Charlie Boone & Vivien Measday, "Identification of RCN1 and RSA3 as ethanol-tolerant genes in *Saccharomyces cerevisiae* using a high copy barcoded library," *FEMS Yeast Research,* vol. 12, no. 1, p. 48–60, February 2012.

[32] V. Costa, M. A. Amorim, E. Reis, A. Quintanilha and P. Moradas-Ferreira, "Mitochondria1 superoxide disrnutase is essential for ethanol tolerance of *Saccharomyces cerevisiae* in the post-diauxic phase," *Microbiology,* vol. 143, pp. 1649-1656, May 1997.

[33] Emel Arinc, Haydar Lelik, "Biochemical Characteristics of Purified Beef Liver NADPH–Cytochrome P450 Reductase," *Journal of Biochemical and Molecular Toxicology,* vol. 16, no. 6, pp. 286-297, December 2002.

[34] Jidong Liu, Yibo Zhu, Guocheng Du, Jingwen Zhou, Jian Chen, "Response of *Saccharomyces cerevisiae* to D-limonene-induced oxidative stress," *Applied Microbial and Cell Physiology ,* vol. 97, no. 14, p. 6467–6475, July 2013.

[35] Timothy C. R. Brennan, Jens O. Krömer, Lars K. Nielsena, "Physiological and Transcriptional Responses of *Saccharomyces cerevisiae* to d-Limonene Show Changes to the Cell Wall but Not to the Plasma Membrane," *Applied and Environmental Microbiology,* vol. 79, no. 12, p. 3590–3600, June 2013.

[36] Sjef Cornelissen, Shanshan Liu, Amit Tatyasaheb Deshmukh, Andreas Schmid, Bruno Bühler, "Cell physiology rather than enzyme kinetics can determine the efficiency of cytochrome P450-catalyzed C–H-oxyfunctionalization," *Journal of Industrial Microbiology & Biotechnology,* vol. 38, no. 9, p. 1359–1370, September 2011.

[37] Yuchun Du, Jianhong Zhou, Jinjiang Fan, Zhiyuan Shen, and Xian Chen, "Streamline Proteomic Approach for Characterizing Protein-Protein Interaction Network in a *RAD52* Protein Complex," *Journal of Proteome Research,* vol. 8, no. 5, p. 2211–2217, May 2009.

[38] Adam L. Hughes, David W. Powell, Martin Bard, James Eckstein, Robert Barbuch, Andrew J. Link, and Peter J. Espenshade, "Dap1/PGRMC1 Binds and Regulates Cytochrome P450 Enzymes," *Cell Metabolism,* vol. 5, p. 143–149, February 2007.